GEOLOGICA CARPATHICA, AUGUST 2013, 64, 4, 327–351 doi: 10.2478/geoca-2013-0023

K-Ar and Rb-Sr geochronology and evolution of the Štiavnica Stratovolcano (Central Slovakia)

IGOR V. CHERNYSHEV[1], VLASTIMIL KONEČNÝ[2], JAROSLAV LEXA[3], VLADIMIR A. KOVALENKER[1], STANISLAV JELEŇ[4,5], VLADIMIR A. LEBEDEV[1] and YURIJ V. GOLTSMAN[1]

[1]Institute of Geology of Ore Deposits, Petrography, Mineralogy and Geochemistry, Russian Academy of Sciences, Staromonetny per. 35, 119 017 Moscow, Russian Federation; kva@igem.ru
[2]State Geological Institute of Dionýz Štúr, Mlynská dolina 1, 817 04 Bratislava, Slovak Republic; vlasto.konecny@gmail.com
[3]Geological Institute, Slovak Academy of Sciences, Dúbravská cesta 9, 840 05 Bratislava, Slovak Republic; jaroslav.lexa@savbb.sk
[4]Geological Institute, Slovak Academy of Sciences; Branch: Ďumbierska 1, 974 01 Banská, Bystrica, Slovak Republic; jelen@savbb.sk
[5]Faculty of Natural Sciences, Matej Bel University, Tajovského 40, 974 01 Banská Bystrica, Slovak Republic

(Manuscript received June 11, 2012; accepted in revised form March 14, 2013)

Abstract: The Štiavnica Stratovolcano in Central Slovakia is the largest volcano in the Neogene to Quaternary Carpathian volcanic arc. A large caldera, an extensive subvolcanic intrusive complex and a resurgent horst with late stage rhyolite volcanites are the most characteristic features. The results of new K-Ar and Rb-Sr isotope dating using more sophisticated methodical approaches have changed our view on the timing of volcanic and intrusive activity. K-Ar dating of groundmass fractions combined with Rb-Sr isochron dating in the cases of possible rejuvenation has provided highly reliable results. The lifespan of the stratovolcano is apparently shorter than assumed earlier. Evolution of the stratovolcano took place in five stages during the Early Badenian to beginning of Early Pannonian time: (1) construction of the extensive andesite stratovolcano during the interval 15.0–13.5 Ma; (2) denudation of the volcano concluded with the initial subsidence of a caldera and the contemporaneous emplacement of a subvolcanic intrusive complex of diorite, granodiorite, granodiorite porphyries and quartz-diorite porphyries during the interval 13.5–12.9 Ma; (3) subsidence of the caldera and its filling by differentiated andesites during the interval 13.1–12.7 Ma — volcanic activity overlapping with the emplacement of the youngest intrusions; (4) renewed explosive and effusive activity of less differentiated andesites during the interval 12.7–12.2 Ma; (5) uplift of the resurgent horst in the central part of the caldera accompanied by rhyolite volcanic/intrusive activity during the interval 12.2–11.4 Ma. Extensive epithermal mineralization was contemporaneous with the uplift of the resurgent horst and rhyolite volcanic activity and continued till 10.7 Ma.

Key words: Central Slovakia, evolution, resurgent horst, andesite stratovolcano, caldera, K-Ar and Rb-Sr isotope dating, subvolcanic intrusions, rhyolite.

Introduction

The Štiavnica Stratovolcano in Central Slovakia is the largest volcano among Neogene to Quaternary volcanoes at the inner side of the Carpathian arc. Despite a long lasting denudation, rocks of the volcano still cover the area of 2200 km^2. It shows a complex structure involving differentiated rocks, an extensive multiple stage subvolcanic intrusive complex, a caldera 18×22 km and a late stage resurgent horst accompanied by rhyolite volcanic activity. The central zone of the volcano hosts rich intrusion-related and epithermal base/precious metal mineralizations that have been the basis for a long lasting mining tradition and for the rise of the famous medieval mining city of Banská Štiavnica.

Evolution of the stratovolcano took place in five stages during the Early Badenian to Early Pannonian time. While the succession of volcanic formations, subvolcanic intrusive rocks and related metallogenetic processes is quite well established (Konečný et al. 1983, 1998; Lexa et al. 1999a; Koděra & Lexa 2003), the exact timing and duration of volcanic, intrusive and hydrothermal activity remains uncertain. Available biostratigraphic data, including extensive palynology records (Planderová in Konečný et al. 1983; Planderová 1990) and isotope dating results are often contradictory due to remaining problems in the chronostratigraphic assignment of lithostratigraphic units, in the correlation of Paratethys stratigraphic stages with isotope ages, in the complexity of isotope data interpretation in areas of repeated magmatic activity and hydrothermal alterations, and also due to a rather low quality of some of the past isotope datings.

Uncertainty in the timing and duration of volcanic, intrusive and hydrothermal activities has been a reason for additional effort based on more advanced and sophisticated methods of isotope dating and their interpretation. As the outcome of the effort we present an updated evolutionary scheme of the Štiavnica Stratovolcano based on new results of K-Ar and Rb-Sr isotope dating, critical evaluation of available biostratigraphic data and published results of previous isotope dating.

Correlation of biostratigraphic and isotope chronology data is based on the chronostratigraphic assignment of relevant lithostratigraphic units by Kováč et al. (2005) and the newest version of the isotope time scale for the central and eastern Paratethys by Harzhauser & Piller (2007). The relevant time intervals are as follows: Early Badenian 16.3–13.65 Ma, Late Badenian 13.65–12.7 Ma (two-fold division of the Badenian is accepted as definition of the Middle Badenian is problematic; Kováč et al. 2005), Sarmatian 12.7–11.6 Ma (Early and Late Sarmatian are well defined only in the Eastern Paratethys with boundary at 12.0 Ma), Pannonian 11.6–7.2 Ma (with boundaries Early/Middle and Middle/Late Pannonian at 10.5 Ma and 9.0 Ma, respectively; Kováč et al. 2005), Pontian 7.2–5.3 Ma.

Structure of the stratovolcano and stages of volcanic and intrusive activity

The Štiavnica Stratovolcano occupies the SW part of the Central Slovakia Neogene Volcanic Field (Fig. 1). It is the largest as well as the most complex volcano of the field. Its volcanic products extend over an area exceeding 2000 km^2. At the outskirts its rocks overlap mutually with rocks of neighboring stratovolcanoes — Javorie Stratovolcano in the east, stratovolcanoes of Kremnické vrchy mountain range in the north and Vtáčnik Stratovolcano in the northwest. Most of the volcano evolved in a terrestrial environment and volcanic facies grade in the distal zone into volcano-sedimentary complexes that were laid down in the ephemeral stream, fluvial, and/or limnic environments (Fig. 2). However, in the south volcanic products reached the coastal zone of an epi-continental sea, so volcanic facies in the distal zone grade into volcano-sedimentary complexes laid down in the littoral and sublittoral marine environments.

The structure and evolutionary stages of the Štiavnica Stratovolcano have already been described in greater detail elsewhere (Konečný et al. 1995, 1998). Here we present a summary as a basis for the discussion on the timing of volcanic activity. The main structural units of the stratovolcano correspond to five essential stages distinguished in its evolution (Konečný 1970, 1971; Konečný et al. 1995, 1998; Konečný & Lexa 2001): (1) the lower structural unit representing products of the first, pre-caldera stage andesite volcanic activity; (2) the subvolcanic/intravolcanic intrusive complexes that were emplaced during a break in volcanic activity (the second stage); (3) the middle structural unit representing products of the third, caldera stage volcanic activity of differentiated rocks, filling the caldera and paleovalleys on the slopes of the stratovolcano; (4) the upper structural unit representing products of the fourth, post-caldera stage andesite volcanic activity; (5) the *Jastrabá Formation* representing products of the fifth, late-stage rhyolite volcanic activity associated with the uplift of the resurgent horst. Rocks of the lower structural unit rest variably directly on pre-Neogene basement, pre-volcanic sedimentary rocks and/or early volcanic products of garnet-bearing andesites. Succession of units/stages is based on superposition and major unconformities established by geological mapping and sporadic biostratigraphic data including evaluation of palynomorphs. The results of previous isotopic dating are reviewed in the discussion.

The terms complex and formation are used in the text to designate both formal lithostratigraphic units, in which case they are written in italics with capitalized first letters,

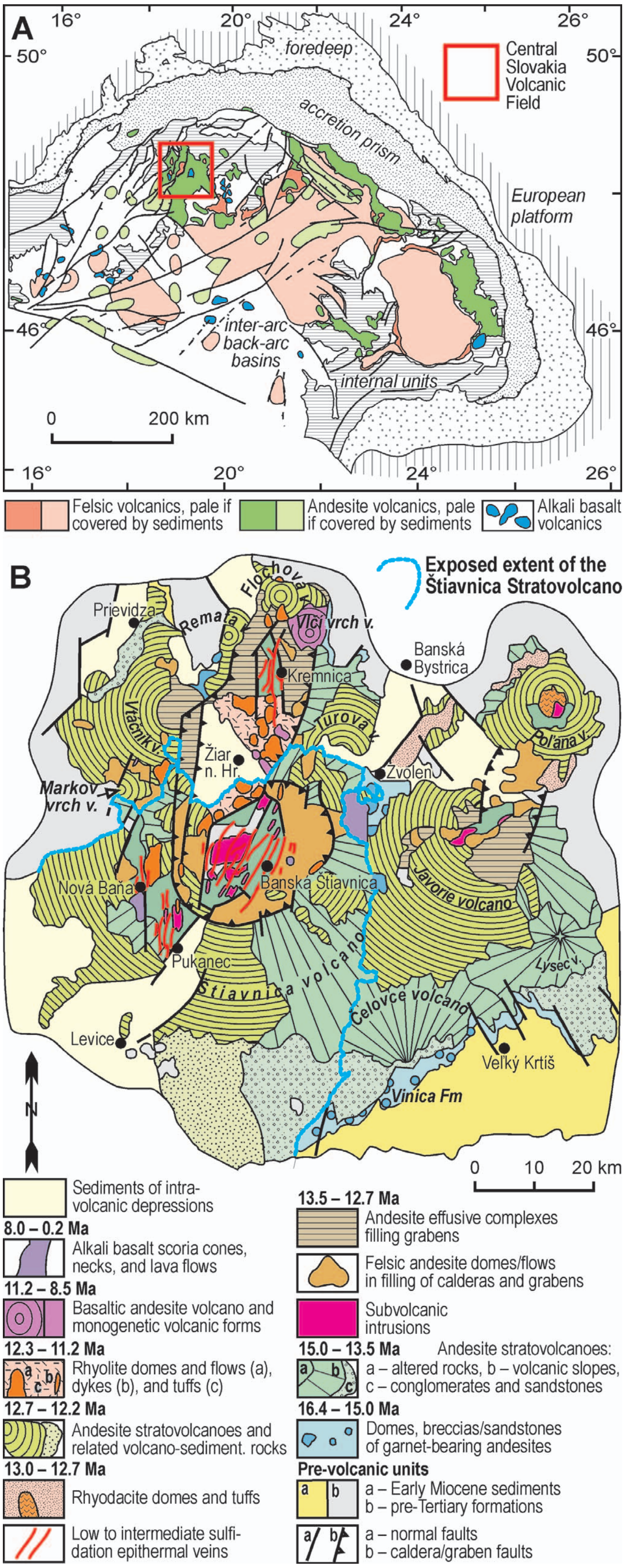

Fig. 1. Position of the Štiavnica Stratovolcano in the structural framework of the Carpathian arc and Pannonian Basin (**A**) and in the structural scheme of the Central Slovakia Neogene Volcanic Field (**B**). Modified after Konečný et al. (1995) and Pécskay et al. (2006).

and informal units (complexes) describing groups of rocks at variable hierarchal levels.

Volcanic formations preceding the Štiavnica Stratovolcano

Evolution of the stratovolcano itself was preceded by volcanic activity of garnet-bearing hypersthene-amphibole andesites at dispersed volcanic centers. Groups of extrusive domes are associated with accumulations of breccias in their surroundings and reworked material in the distal zone. Volcanic activity occurred in the time of the initial stage of back-arc extension in the area of the Central Slovakia Neogene Volcanic Field that gave rise to horsts and grabens and caused a marine transgression. A complex of garnet-bearing andesite extrusive domes and volcaniclastic rocks cropping out between the Javorie and Štiavnica Stratovolcanoes has been defined as the *Neresnica Formation* (Konečný et al. 1983).

Lower structural unit — the first stage

The first stage in the evolution of the stratovolcano corresponds to rocks of the lower structural unit. This unit comprises pyroxene and hornblende-pyroxene andesite stratovolcanic complexes/formations of the Badenian volcanic activity that took place before the caldera subsidence. Paleovolcanic reconstruction reveals remnants of a large stratovolcano, over 40 km in diameter, surrounded by accumulations of epiclastic volcanic rocks. Rocks of the lower structural unit are often covered by younger volcanic products of the caldera and post-caldera stages (Fig. 2).

In the central zone of the stratovolcano the lower structural unit is exposed in the eastern half of the resurgent horst (Figs. 2, 3). Here, the former stratovolcano has been deeply eroded and the lower structural unit consists of pyroxene, amphibole-pyroxene and biotite-amphibole-pyroxene andesite porphyry sills and laccoliths that crop out in the lower part of the andesite stratovolcanic complex.

In the proximal zone (outside of the caldera), the pre-caldera stage stratovolcanic complexes of the lower structural unit are not uniform. Mutual age relationships among rocks exposed in different sectors of the stratovolcano are not known. In the northeast, the lower part of the exposed stratovolcanic complex consists of biotite-amphibole-pyroxene andesites, while the upper part consists mostly of pyroxene andesites. The complex also hosts a large biotite-bearing hornblende-pyroxene andesite porphyry laccolith.

In the western sector pyroxene and amphibole-pyroxene andesite lava flows dominate over sporadic epiclastic volcanic breccias. At the lowermost part of the volcanic complex there are glassy and leucocratic pyroxene andesites accompanied by hyaloclastite breccias. In the borehole PKŠ-1 Gondovo rocks of the first stage rest on marine sedimentary rocks of the late Early Badenian age (Brestenská in Karolus et al. 1975). Closer to the central zone, the complex of lava flows has been invaded by andesite porphyry sills and laccoliths, as well as pyroxene-amphibole andesite extrusive domes.

Several volcanic formations have been distinguished in the lower structural unit in the south-eastern sector of the stratovolcano (Figs. 4, 5). The oldest effusive complex of pyroxene andesites is locally covered by hypersthene-amphibole andesite extrusive domes and related pyroclastic flows and epiclastic volcanic breccias. Both are covered by a slightly younger extensive stratovolcanic complex of amphibole-pyroxene andesite lava flows, extrusive domes, pyroclastic flows and epiclastic volcanic breccias of the *Sebechleby Formation*. The formation extends southward into the marine environment where it comprises laharic breccias, conglomerates and sandstones that alternate eventually with fauna-bearing marine sedimentary rocks (Fig. 4). Mafic pyroxene andesite lava flows of the *Žibritov Effusive Complex* conclude the succession of the lower structural unit in the SE sector of the stratovolcano.

It follows that the first, pre-caldera stage in evolution of the stratovolcano involved a gradual formation of a large andesite stratovolcano with related aprons of epiclastic volcanic rocks. Generally, the early activity of dominantly pyroxene andesites was followed by activity of more evolved and often porphyritic amphibole-pyroxene, pyroxene-amphibole and biotite amphibole-pyroxene andesites (Figs. 4, 5). However, mafic pyroxene andesites also appeared among the youngest volcanic products of the first stage. During maturity of the first stage stratovolcano, emplacement of extrusive domes, diorite porphyry intrusions and andesite to andesite porphyry sills and laccoliths took place, with the exception of the extrusive domes preferentially into the lower parts of volcanic complex in the central and proximal zones of the stratovolcano.

The south distal zone of the stratovolcano evolved in a shallow marine environment (Konečný et al. 1998) and biostratigraphic evidence is available for timing of the beginning of volcanic activity. In the borehole PKŠ-1 Gondovo in the SW sector of the stratovolcano (Fig. 2), the beginning of volcanic activity is recorded by reworked pumice tuffs at the depth of 822.4 m covered by breccias and lava flows of the lower structural unit (Karolus et al. 1975). Fauna in underlying marine sedimentary rocks points to the uppermost Lower to lowermost Upper (?) Badenian stage (Brestenská in Karolus et al. 1975). In the borehole ŠV-8 (Dolné Semerovce) tuffaceous sediments corresponding to the first stage of the Štiavnica Stratovolcano occur in the interval 194–430 m (Fig. 2). Macrofauna, foraminifera, palynomorphs and calcareous nannofossils at the interval 270–430 m imply the late Early Badenian age (Zone NN5), while in the interval 194–270 m they imply the early Late Badenian age (beginning of the Zone NN6) (Vass et al. 1981; Ozdínová 2008). In the borehole GK-3 Horné Rykynčice in the southern sector of the stratovolcano (Fig. 2), the beginning of volcanic activity is recorded by reworked pumice tuffs in marine sedimentary rocks at the depth of 618 m covered by pyroclastic flow breccia and a complex of epiclastic volcanic breccias, conglomerates and sandstones representing the distal zone of the first stage andesite stratovolcano (Konečný et al. 1966). Palynological evidence from underlying marine sedimentary rocks with reworked material of garnet-bearing andesites points to the Early Badenian age (Planderová in Konečný et al. 1983). Middle to late Early Badenian age is implied by microfauna and palynomorphs in marine siltstones interbedded with epiclastic volcanic sandstones in the interval 237–0 m (Lehotayová in Konečný et al. 1966; Brestenská et al. 1980;

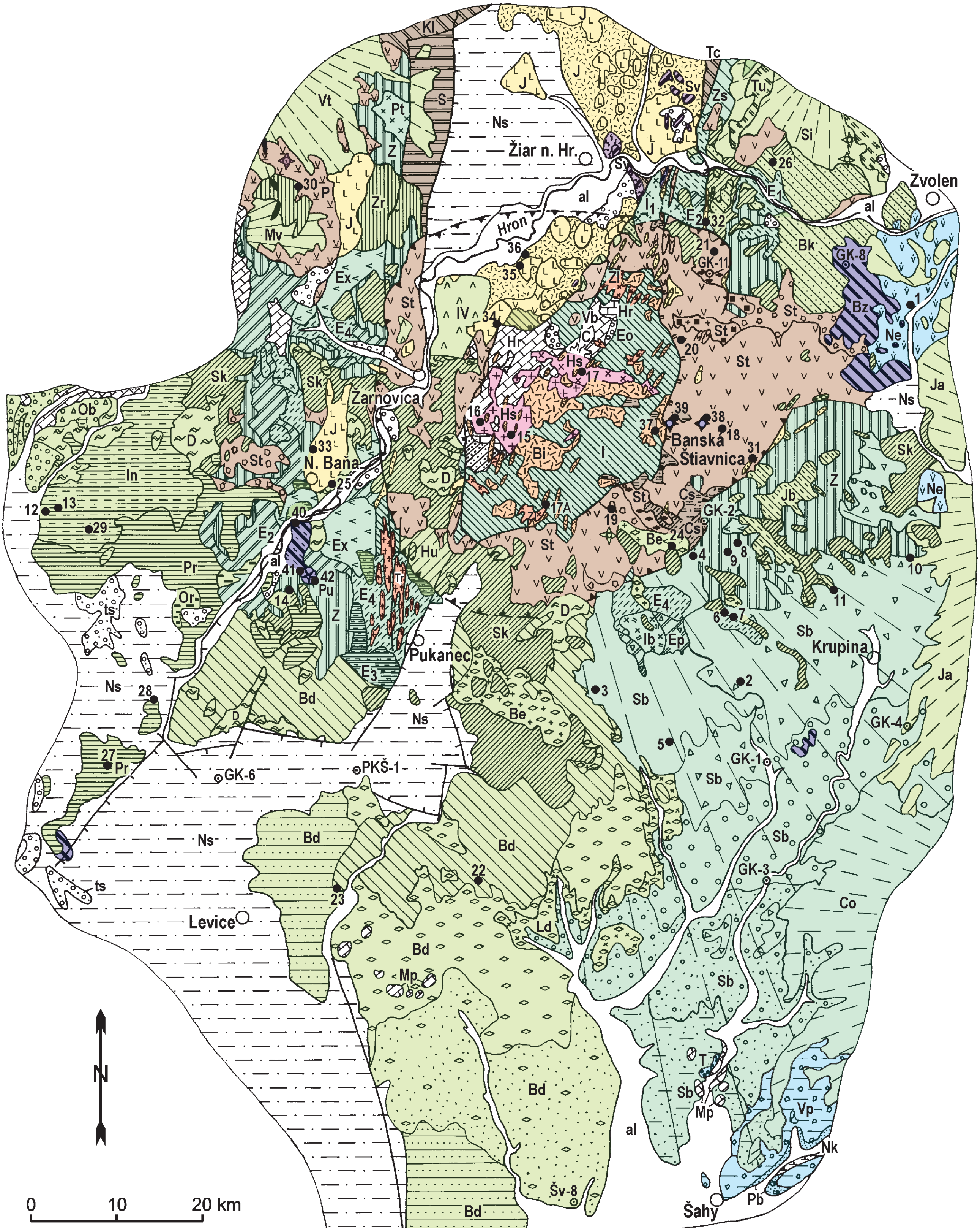

Fig. 2. Structural scheme of the Štiavnica Stratovolcano including localization of samples. Modified after Konečný & Lexa 2001. *The legend is on the next page.*

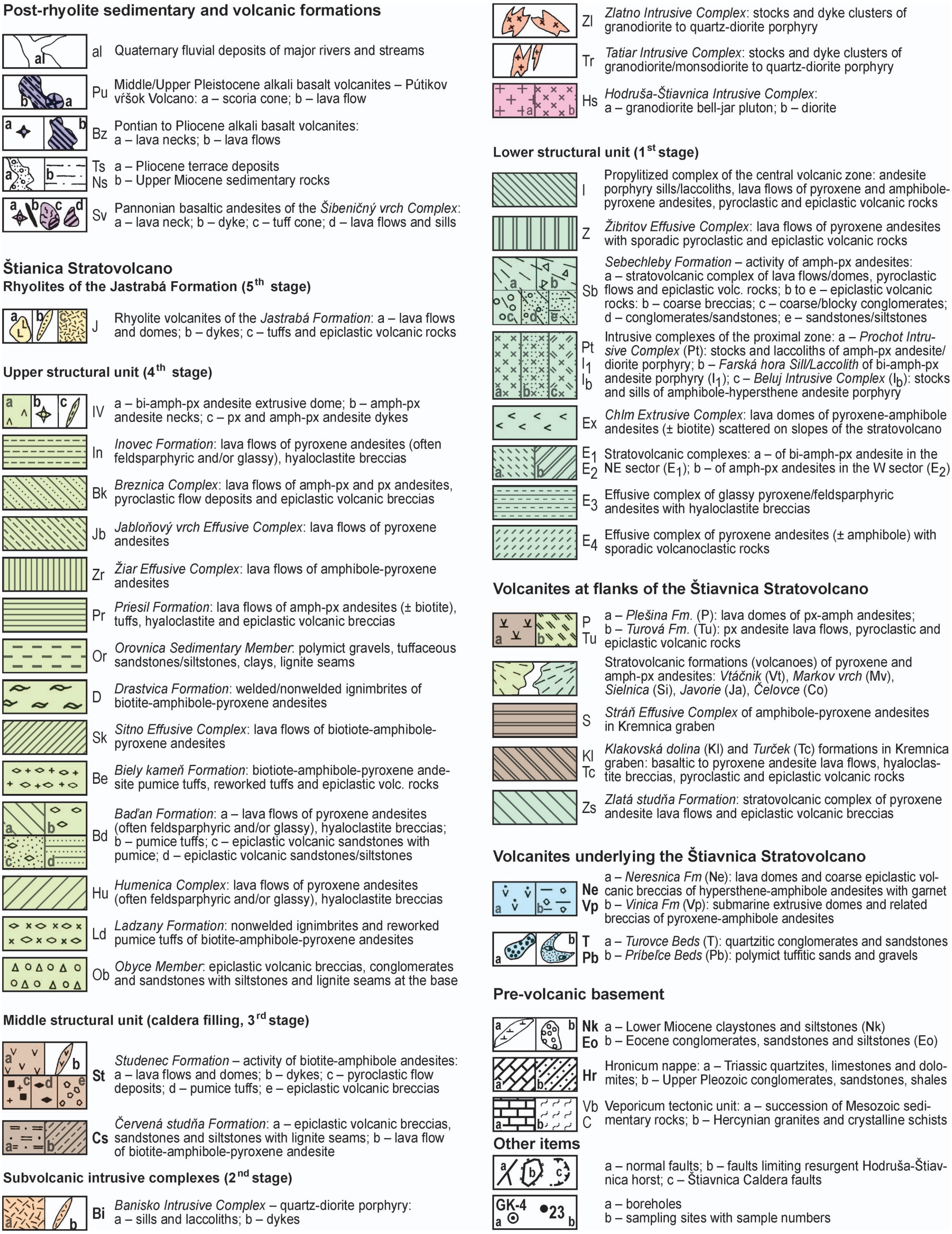
Post-rhyolite sedimentary and volcanic formations
al Quaternary fluvial deposits of major rivers and streams
Pu Middle/Upper Pleistocene alkali basalt volcanites – Pútikov vŕšok Volcano: a – scoria cone; b – lava flow
Bz Pontian to Pliocene alkali basalt volcanites: a – lava necks; b – lava flows
Ts a – Pliocene terrace deposits
Ns b – Upper Miocene sedimentary rocks
Sv Pannonian basaltic andesites of the Šibeničný vrch Complex: a – lava neck; b – dyke; c – tuff cone; d – lava flows and sills
Štianica Stratovolcano
Rhyolites of the Jastrabá Formation (5th stage)
J Rhyolite volcanites of the Jastrabá Formation: a – lava flows and domes; b – dykes; c – tuffs and epiclastic volcanic rocks
Upper structural unit (4th stage)
IV a – bi-amph-px andesite extrusive dome; b – amph-px andesite necks; c – px and amph-px andesite dykes
In Inovec Formation: lava flows of pyroxene andesites (often feldsparphyric and/or glassy), hyaloclastite breccias
Bk Breznica Complex: lava flows of amph-px and px andesites, pyroclastic flow deposits and epiclastic volcanic breccias
Jb Jabloňový vrch Effusive Complex: lava flows of pyroxene andesites
Zr Žiar Effusive Complex: lava flows of amphibole-pyroxene andesites
Pr Priesil Formation: lava flows of amph-px andesites (± biotite), tuffs, hyaloclastite and epiclastic volcanic breccias
Or Orovnica Sedimentary Member: polymict gravels, tuffaceous sandstones/siltstones, clays, lignite seams
D Drastvica Formation: welded/nonwelded ignimbrites of biotite-amphibole-pyroxene andesites
Sk Sitno Effusive Complex: lava flows of biotiote-amphibole-pyroxene andesites
Be Biely kameň Formation: biotiote-amphibole-pyroxene andesite pumice tuffs, reworked tuffs and epiclastic volc. rocks
Bd Baďan Formation: a – lava flows of pyroxene andesites (often feldsparphyric and/or glassy), hyaloclastite breccias; b – pumice tuffs; c – epiclastic volcanic sandstones with pumice; d – epiclastic volcanic sandstones/siltstones
Hu Humenica Complex: lava flows of pyroxene andesites (often feldsparphyric and/or glassy), hyaloclastite breccias
Ld Ladzany Formation: nonwelded ignimbrites and reworked pumice tuffs of biotite-amphibole-pyroxene andesites
Ob Obyce Member: epiclastic volcanic breccias, conglomerates and sandstones with siltstones and lignite seams at the base
Middle structural unit (caldera filling, 3rd stage)
St Studenec Formation – activity of biotite-amphibole andesites: a – lava flows and domes; b – dykes; c – pyroclastic flow deposits; d – pumice tuffs; e – epiclastic volcanic breccias
Cs Červená studňa Formation: a – epiclastic volcanic breccias, sandstones and siltstones with lignite seams; b – lava flow of biotite-amphibole-pyroxene andesite
Subvolcanic intrusive complexes (2nd stage)
Bi Banisko Intrusive Complex – quartz-diorite porphyry: a – sills and laccoliths; b – dykes
Zl Zlatno Intrusive Complex: stocks and dyke clusters of granodiorite to quartz-diorite porphyry
Tr Tatiar Intrusive Complex: stocks and dyke clusters of granodiorite/monsodiorite to quartz-diorite porphyry
Hs Hodruša-Štiavnica Intrusive Complex: a – granodiorite bell-jar pluton; b – diorite
Lower structural unit (1st stage)
I Propylitized complex of the central volcanic zone: andesite porphyry sills/laccoliths, lava flows of pyroxene and amphibole-pyroxene andesites, pyroclastic and epiclastic volcanic rocks
Z Žibritov Effusive Complex: lava flows of pyroxene andesites with sporadic pyroclastic and epiclastic volcanic rocks
Sb Sebechleby Formation – activity of amph-px andesites: a – stratovolcanic complex of lava flows/domes, pyroclastic flows and epiclastic volc. rocks; b to e – epiclastic volcanic rocks: b – coarse breccias; c – coarse/blocky conglomerates; d – conglomerates/sandstones; e – sandstones/siltstones
Pt I1 Ib Intrusive complexes of the proximal zone: a – Prochot Intrusive Complex (Pt): stocks and laccoliths of amph-px andesite/diorite porphyry; b – Farská hora Sill/Laccolith of bi-amph-px andesite porphyry (I1); c – Beluj Intrusive Complex (Ib): stocks and sills of amphibole-hypersthene andesite porphyry
Ex Chlm Extrusive Complex: lava domes of pyroxene-amphibole andesites (± biotite) scattered on slopes of the stratovolcano
E1 E2 Stratovolcanic complexes: a – of bi-amph-px andesite in the NE sector (E1); b – of amph-px andesites in the W sector (E2)
E3 Effusive complex of glassy pyroxene/feldsparphyric andesites with hyaloclastite breccias
E4 Effusive complex of pyroxene andesites (± amphibole) with sporadic volcanoclastic rocks
Volcanites at flanks of the Štiavnica Stratovolcano
P Tu a – Plešina Fm. (P): lava domes of px-amph andesites; b – Turová Fm. (Tu): px andesite lava flows, pyroclastic and epiclastic volcanic rocks
Stratovolcanic formations (volcanoes) of pyroxene and amph-px andesites: Vtáčnik (Vt), Markov vrch (Mv), Sielnica (Si), Javorie (Ja), Čelovce (Co)
S Stráň Effusive Complex of amphibole-pyroxene andesites in Kremnica graben
Kl Tc Klakovská dolina (Kl) and Turček (Tc) formations in Kremnica graben: basaltic to pyroxene andesite lava flows, hyaloclastite breccias, pyroclastic and epiclastic volcanic rocks
Zs Zlatá studňa Formation: stratovolcanic complex of pyroxene andesite lava flows and epiclastic volcanic breccias
Volcanites underlying the Štiavnica Stratovolcano
Ne Vp a – Neresnica Fm (Ne): lava domes and coarse epiclastic volcanic breccias of hypersthene-amphibole andesites with garnet b – Vinica Fm (Vp): submarine extrusive domes and related breccias of pyroxene-amphibole andesites
T Pb a – Turovce Beds (T): quartzitic conglomerates and sandstones b – Príbelce Beds (Pb): polymict tuffitic sands and gravels
Pre-volcanic basement
Nk Eo a – Lower Miocene claystones and siltstones (Nk) b – Eocene conglomerates, sandstones and siltstones (Eo)
Hr Hronicum nappe: a – Triassic quartzites, limestones and dolomites; b – Upper Pleozoic conglomerates, sandstones, shales
Vb C Veporicum tectonic unit: a – succession of Mesozoic sedimentary rocks; b – Hercynian granites and crystalline schists
Other items
a – normal faults; b – faults limiting resurgent Hodruša-Štiavnica horst; c – Štiavnica Caldera faults
GK-4 •23
a – boreholes
b – sampling sites with sample numbers

Fig. 2. Legend.

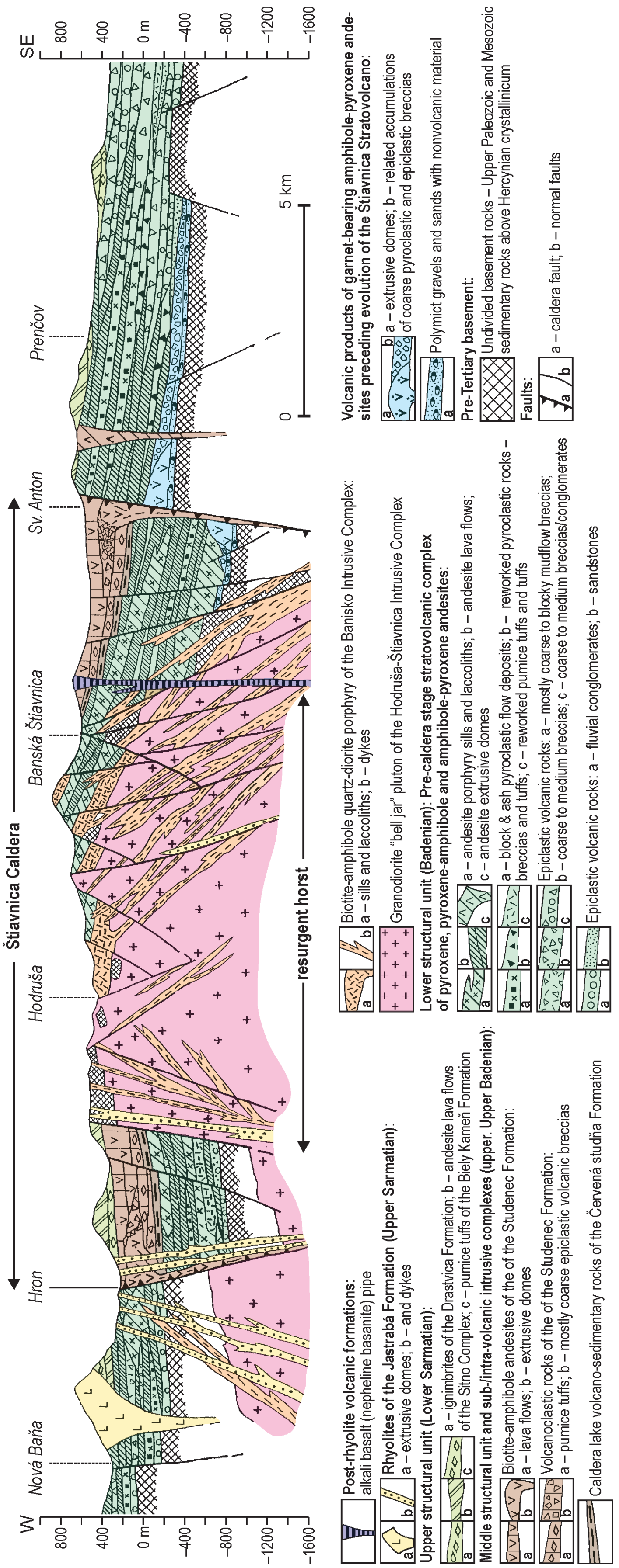

Fig. 3. Section of the Štiavnica Caldera and Hodruša-Štiavnica resurgent horst. Modified after Konečný & Lexa 2001.

Planderová in Konečný et al. 1983). Overlying epiclastic volcanic breccias and conglomerates belong to the *Sebechleby Formation.*

Subvolcanic/intravolcanic intrusive complexes — the second stage

The second stage in the evolution of the Štiavnica Stratovolcano corresponded to a long lasting break in volcanic activity and extensive denudation of the former stratovolcano down to a thickness of 500–1000 m. In the SW sector of the stratovolcano the break in volcanic activity is indicated by shallow marine tuffaceous sedimentary rocks that rest on top of the *Sebechleby Formation* (first stage) and are covered by pumice tuffs of the Lower Sarmatian *Ladzany Formation* (fourth stage). In the borehole ŠV-8 Dolné Semerovce (Vass et al. 1981) (Fig. 2) they are represented by marly clays and sandy clays with tuffitic intercalations in the interval 21–194 m. Macrofauna, foraminifera, palynomorphs and calcareous nannofossils at this interval imply the Upper Badenian stage (Zone NN6) (Vass et al. 1981; Ozdínová 2008). The period of denudation was concluded by the initial subsidence in the central part of the stratovolcano, giving rise to local depressions with lacustrine and/or limnic environments. Related volcano-sedimentary deposits of the *Červená studňa Formation* are described as a part of the middle structural unit below. Palynology has confirmed the uppermost Upper Badenian stage (Planderová in Konečný et al. 1983).

However, the break in volcanic activity did not represent a break in magmatic activity. Evolution of magma in a shallow magma chamber (Lexa et al. 1998b; Konečný 2002) led to a repeated emplacement of extensive subvolcanic/intravolcanic intrusive bodies and complexes. These crop out in the uplifted block of the resurgent horst, in the central zone of the stratovolcano (Figs. 2, 3). The age of subvolcanic intrusions is not equally constrained. Taking into account mutual crosscutting their emplacement took place in the following order (Konečný et al. 1993, 1998; Konečný & Lexa 2001):

The oldest *Hodruša-Štiavnica Intrusive Complex,* that crops out in the central part of the resurgent horst comprises an older diorite subvolcanic intrusion and a younger granodiorite bell-jar pluton that extends over an area of 100 km^2. Both intrusions invaded basement rocks underlying the volcanic complex.

Granodiorite to quartz-diorite porphyry dyke clusters and small stocks of the *Zlatno Intrusive Complex* situated at the periphery of the granodiorite pluton postdate the pluton.

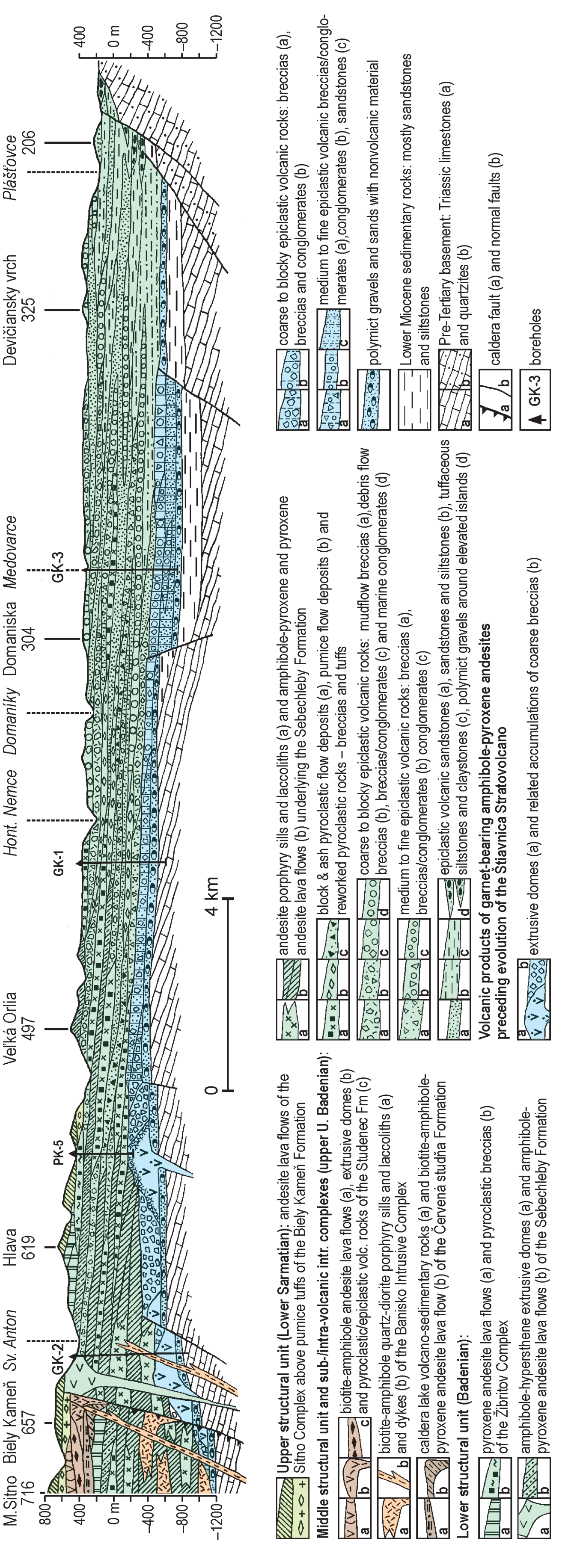

Fig. 4. Schematic section of the lower structural unit in the SE sector of the Štiavnica Stratovolcano. Modified after Konečný & Lexa 2001.

Stocks in basement rocks pass upward into dyke clusters that are emplaced in andesites and andesite porphyries of the lower structural unit.

Diorite to quartz-diorite porphyry sills and dykes of the *Banisko Intrusive Complex* show some features that are characteristic of ring dykes. They have invaded major discontinuities in the basement, the granodiorite pluton, the contact between basement and volcanic complex and the overlying volcanic complex of the lower structural unit. The highest level sills have reached the lower part of the caldera filling. Outward dipping dykes show a preferential orientation in the directions N-S to NE-SW.

All the intrusions are younger than andesites and andesite porphyries of the first stage. Their relationship to the caldera filling of the third stage is not known with one exception — quartz-diorite porphyry sills and dykes of the youngest *Banisko Intrusive Complex* are also emplaced in the lowermost parts of the caldera filling. That implies a partial overlap among the second and third stages.

Middle structural unit (caldera filling) — the third stage

The third stage is also called the caldera stage. During this stage the Štiavnica Stratovolcano Caldera subsided and was filled by differentiated rocks of biotite-hornblende andesite to dacite composition. The caldera 18×22 km is of a oval form (Fig. 2). The extent of its subsidence is estimated at 500 m. At the base of the caldera filling there are lacustrine and limnic sediments of the *Červená studňa Formation* — reworked tuffs, fine epiclastic volcanic breccias and sandstones, siltstones and tuffaceous clays including lignite seams. Close to the margins of the caldera, the formation also includes coarse epiclastic volcanic breccias and a single biotite-amphibole-pyroxene andesite lava flow in the south.

The caldera is filled with rocks of the *Studenec Formation* comprising biotite-amphibole andesite to amphibole-biotite dacite extrusive domes, dome flows, pyroclastic flow breccias, ignimbrites and epiclastic volcanic breccias (Figs. 3, 5). The early stage of the subsidence associated with explosive activity that gave rise to pumice fall and pumice flow deposits that along with reworked tuffs and epiclastic volcanic sandstones/siltstones rest upon sedimentary rocks of the *Červená studňa Formation* (Figs. 4, 5). Subsequent extrusive activity filled the caldera with extrusive domes, domeflows, pyroclastic flow breccias and related coarse epiclastic volcanic breccias of the *Studenec Formation* 350–500 m in thickness. Remaining local morphological depressions hosted marshes and temporary lakes giving rise to overlying horizons of the lacustrine and limnic type deposits with diatomaceous earth and/or silicite intercalations.

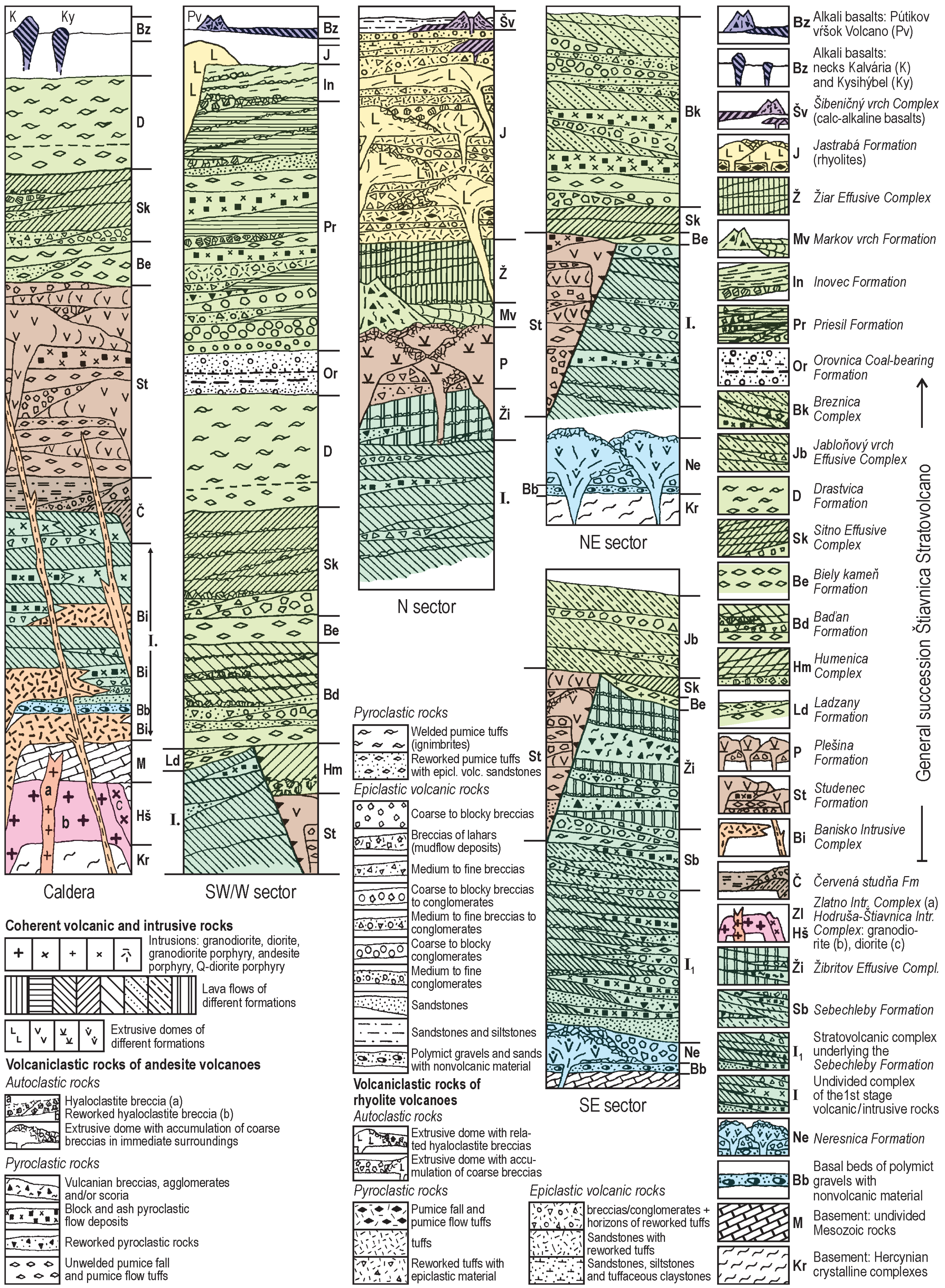

Fig. 5. Stratigraphic columns in different sectors of the Štiavnica Stratovolcano.

Where former paleovalleys were cut off by the caldera fault, the caldera walls were rather low and products of the caldera-related volcanic activity passed over on the slopes of the stratovolcano filling the paleovalleys up to a thickness of 200 meters (mostly thick lava flows, pyroclastic flow deposits and epiclastic volcanic breccias). At the foot of the stratovolcano epiclastic volcanic rocks in filling of the paleovalleys passed outward into distal facies ephemeral stream, lacustrine and limnic deposits, including locally lignite seams (Obyce lignite deposit at west, Zvolenská kotlina Basin at northeast) (Fig. 2).

There are no marine sedimentary rocks interbedded with rocks of the *Studenec Formation* and no biostratigraphic data based on marine fauna are available. Palynomorphs in lacustrine siltstones and claystones at the base and top of the *Studenec Formation* in the caldera as well as in sediments interbedded with distal facies rocks at the outskirts of the stratovolcano point to the time interval: end of Late Badenian — beginning of Early Sarmatian (Planderová in Konečný et al. 1983). Macroflora in diatomaceous limnic deposits overlying caldera filling in its northern part has been assigned to the Lower Sarmatian (Sitár 1973).

Upper structural unit — the fourth stage

The unit comprises andesite explosive, stratovolcanic and effusive volcanic complexes and formations that represent volcanic activity post-dating the caldera subsidence and predating the uplift of the resurgent horst and related rhyolitic volcanic activity. Individual complexes/formations are spatially limited to certain sectors of the volcano (Fig. 2), and often separated by short periods of erosion. Relevant volcanic centers were situated on slopes of the stratovolcano, along the caldera margin and inside the caldera. Volcanic rocks covered the caldera, accumulated in paleovalleys on slopes of the stratovolcano and spread into broader accumulations at the foot of the stratovolcano. Hyaloclastite breccias and extensive horizons of conglomerates, sandstones and reworked tuffs reveal a shallow marine environment in the southern sector of the stratovolcano.

Accumulation of volcanic rocks in different sectors of the stratovolcano reflected a successive activation of individual volcanic centers. No individual section provides a complete record. A complete succession of formations and complexes is based on the correlation of local stratigraphic columns (Fig. 5) (Konečný et al. 1998): (1) biotite-amphibole-pyroxene andesite pumice tuffs of the *Ladzany Formation*; (2) pyroxene andesite lava flows and related hyaloclastite breccias and epiclastic volcanic conglomerates and sandstones of the *Baďan Formation* and *Humenica Complex*; (3) biotite-amphibole-pyroxene andesite pumice tuffs of the *Biely Kameň Formation*; amphibole-pyroxene andesite lava flows, pyroclastic flow deposits and epiclastic volcanic breccias in the lower part of the *Breznica Complex*; (4) biotite-amphibole-pyroxene andesite lava flows of the *Sitno Effusive Complex* and biotite-amphibole-pyroxene andesite epiclastic breccias in the middle part of the *Breznica Complex*; (5) biotite-amphibole-pyroxene andesite ignimbrites of the *Drastvica Formation*; (6) amphibole-pyroxene andesite lava flows of the *Priesil* and *Žiar Effusive Complexes*; (7) pyroxene andesite lava flows of the *Inovec Formation*, *Jabloňový vrch Complex* and upper part of the *Breznica Complex*.

Distal facies volcanic products of the fourth stage reached a marine environment in the south. Reworked tuffs and tuffaceous sediments corresponding to the *Ladzany* and *Drastvica Formations* include macrofauna of the Early Sarmatian age (Brestenská 1970; Karolus & Váňová 1973). Freshwater lacustrine deposits interbedded with volcanic formations of the fourth stage elsewhere contain remnants of macroflora and palynomorphs pointing to the Early Sarmatian age of the *Baďan Formation* and *Biely Kameň Formation* and *Breznica Complex* (Němejc 1967; Sitár 1973; Planderová in Konečný et al. 1983).

Rhyolites of the Jastrabá Formation — the fifth stage

Rhyolite volcanic activity of the fifth, late stage associated with an uplift of the asymmetric resurgent horst in the center of the caldera and its denudation to the level of basement rocks and with a contemporaneous subsidence of the Žiar Depression at the northern sector of the stratovolcano. We explain these phenomena using the model of Smith & Bailey (1968) for resurgent cauldrons as being caused by a large scale relocation of rhyolite magma from underneath the Žiar Depression to the roots of the resurgent horst and related isostatic equilibration (Konečný 1971; Konečný et al. 1998). The volcanic centers of the rhyolite volcanic activity were situated on marginal faults of the resurgent horst, marginal faults of the Žiar Depression and N-S striking fault systems west of the Žiar Depression (Nová Baňa–Kľak fault system) (Fig. 2).

Products of the rhyolite magmatism (*Jastrabá Formation*) appear as dykes, intrusions and extrusive domes on N-S to NE-SW striking faults. West of the caldera they associate with faults of the Nová Baňa–Kľak volcano-tectonic zone. In the central zone of the Štiavnica Stratovolcano rhyolite dykes and extrusive domes follow marginal faults of the resurgent horst, especially at its western and north-western sides. In the northern sector of the stratovolcano an extensive dome/flow complex with related pyroclastic and epiclastic volcanic rocks spreads along the south-eastern and eastern marginal faults of the Žiar Depression.

Early sporadic extrusive and explosive activity of rhyodacites was followed by a widespread activity of plagioclase and plagioclase-sanidine rhyolites. Products of the late activity of plagioclase-quartz-sanidine rhyolites are found in the northern part of the Žiar Depression interbedded with lacustrine and/or limnic type deposits with horizons of sedimentary and/or hot spring silicites that are related to the outflow of fluids from the Kremnica epithermal system (Koděra et al. 2010). Dark silicites and associated carbonaceous clays are rich in palynomorphs implying the Late Sarmatian to Early Pannonian age (Planderová in Konečný et al. 1983). No other direct biostratigraphic data are available. In the Žiar Depression rhyolite volcanites of the *Jastrabá Formation* rest upon sedimentary rocks of the Upper Sarmatian stage and are covered by sedimentary rocks of the Upper Pannonian and Pontian stages (Konečný et al. 1983; Lexa et al. 1998a).

Post-rhyolite volcanic formations

In the Štiavnica Stratovolcano area there are minor occurrences of younger volcanic activity represented by high alumina and alkali basalts (Fig. 2). High alumina basalt dykes, sills, lava flows and tuff cone of the *Šibeničný vrch Complex* in the surroundings of the town of Žiar nad Hronom postdate rhyolite volcanic activity. Sporadic activity of alkali basalts (nepheline basanites) created two necks east of the town of Banská Štiavnica, extensive lava flows at the eastern base of the stratovolcano and a small volcano, Pútikov vŕšok, next to the town of Nová Baňa to the west. Its lava flows rest upon Quaternary terrace accumulations of the river Hron.

Related ore mineralizations

The Štiavnica Stratovolcano hosts intrusion-related, as well as extensive epithermal base metal, silver and gold mineralizations. Details of metallogeny have been treated extensively elsewhere (e.g. Lexa et al. 1999a; Lexa 2001; references in these papers). Here we refer only to the established relationship between the metallogenetic processes and the structure and evolution of the stratovolcano.

No metallogenetic processes are related to the andesites and andesite porphyries of the lower structural unit. However, rocks of this unit host many of the younger mineralizations.

The diorite intrusion of the *Hodruša-Štiavnica Intrusive Complex* is the parental intrusion of the high sulphidation system of Šobov that is hosted by andesites of the lower structural unit (Onačila et al. 1995; Lexa et al. 1999a,b).

The granodiorite intrusion of the *Hodruša-Štiavnica Intrusive Complex* is the parental body for the magnetite skarn mineralization that affected surrounding carbonate rocks. It is also the parental body as well as the host for the intrusion-related stockwork/disseminated base metal mineralization (Onačila et al. 1995; Koděra et al. 1998, 2004; Lexa et al. 1999a).

The granodiorite to quartz-diorite porphyry stocks and dyke clusters of the *Zlatno Intrusive Complex* are the parental intrusions of the porphyry/skarn Cu ± Au, Mo mineralization at the localities Zlatno, Šementlov, Medené, Kozí potok, Handerlová and Sklené Teplice–Vydričná dolina (Onačila et al. 1995; Lexa et al. 1999a).

The Rozália mine epithermal gold mineralization in Hodruša is hosted by andesites and andesite porphyries of the lower structural unit. It evolved during the early stage of the caldera subsidence, prior to the emplacement of quartz-diorite sills of the *Banisko Intrusive Complex* (Koděra & Lexa 2003; Koděra et al. 2005). The barren hot spring systems of Dekýš and Červená studňa, hosted by rocks of the *Červená studňa Formation* and lower part of the *Studenec Formation*, evolved roughly in the same time interval (Onačila et al. 1995; Lexa 2001).

The Varta high sulphidation system next to the town of Banská Belá is situated in rocks of the *Studenec Formation* filling the caldera. We assume a relationship to the hypothetical porphyry intrusion emplaced during the caldera stage of the stratovolcano.

The extensive system of base metal, silver-base metal and gold-silver epithermal veins is hosted by faults of the resurgent horst. The rather long living system evolved during the uplift of the resurgent horst. Evolution of the system took place during and after the late stage rhyolitic magmatic activity (Kovalenker et al. 1991; Onačila et al. 1995; Chernyshev et al. 1995; Lexa et al. 1999a; Háber et al. 2001; Lexa 2001).

Methodology of the new K-Ar and Rb-Sr isotope dating

K-Ar method

Radiogenic ^{40}Ar content measurements were performed by isotope dilution method with ^{38}Ar as a spike. The MI-1201 IG mass spectrometer with low-blank argon extraction and purification device was used. The overall analytical system was developed and calibrated for young (Neogene–Quaternary) magmatic rock dating (Chernyshev et al. 2002, 2006). Argon isotope analyses were conducted in static regime of mass-spectrometer measurements at resolving power ~1200. The last provided the interference elimination on the 36 m/e mass peak: the argon isotope peak ($^{36}Ar^+$, 35.98 m/e) was resolved from the isobaric peak ($^{12}C_3{}^+$, 36.01 m/e). The overall system sensitivity in argon was 5×10^{-3}A/tor, total blank did not exceed 3×10^{-3} and 1×10^{-5} ng in isotopes ^{40}Ar and ^{36}Ar respectively. The potassium content was determined by the flame spectrophotometry method. In the case of plagioclase monomineral samples having low (<0.5 %) potassium content the isotope dilution method with ^{39}K spike was used. The accuracy was controlled by systematic analyses of the geochronological standard samples Bern-4 (muscovite), P-207 (muscovite) and 1/76 (basalt).

Rb-Sr method

The isotope dilution method with $^{85}Rb+^{84}Rb$ as mixed spike was used to assess Rb and Sr contents. Whole rock and monomineral samples, 10–20 mg in mass, were decomposed in acid and then subjected to Rb and Sr extraction at the column with the Dowex 50×8 (200–400 mesh) anion exchange resin. Rb and Sr mass-spectrometric measurements were performed on the thermal ionization 7-collector Micromass Sector 54 mass-spectrometer. The accuracy was controlled by systematic analyses of the Sr SRM-987 standard sample. The overall errors of the $^{87}Rb/^{86}Sr$ and $^{87}Sr/^{86}Sr$ ratios determination that were used in isochron calculations averaged ±0.5 % and ±0.005 % respectively.

Precision of the K-Ar and Rb-Sr age data

Errors of all isotope age values that are summarized and discussed in the present paper correspond to the $\pm2\ \sigma$ level. They differ for individual samples. Errors of K-Ar ages average around ±3.5 % relative (around ±0.35 Ma in the case of our results) and represent exclusively analytical errors. Roughly ±1.5 % relative of this error value constitutes the error of the potassium content determination. The rest represents the error of the radiogenic ^{40}Ar determination that in turn depends on the sum of mass-spectrometric measurement errors as well as on the non-radiogenic ^{40}Ar content in individual samples. The K-Ar age determination errors were calculated using the formula of Baksi et al. (1967) as recommended by Baksi (1982) for the case of individual Ar isotopes error estimates.

The 2 σ-errors of Rb-Sr isochron ages are less than the errors of K-Ar ages. Their value varies around 0.33 Ma. In this case the error does not represent as much a sum of analytical errors. It is rather given by deviation of data points incorporated into the isochron calculation relative to the isochron regression line.

The following constants recommended by the IUGS Subcomission for Geochronology (Steiger & Jäger 1977) were used in age calculations: $\lambda_\kappa = 0.581 \times 10^{-10}$ year^{-1}, $\lambda_\beta = 4.962 \times 10^{-10}$ year^{-1}, $^{40}K/K = 0.01167$ at. % (K-Ar method) and 1.42×10^{-10} year^{-1}, $^{85}Rb/^{87}Rb = 2.59265$ (Rb–Sr method).

Excess radiogenic argon in young volcanic rocks: rock groundmass as the K-Ar geochronometer

Matsumoto & Kobayashi (1995), Singer et al. (1998) and Chernyshev et al. (1999) have demonstrated that different components inside one rock might be distinct in K-Ar age values. As the initial $^{40}Ar/^{36}Ar$ isotope ratio in geochronological calculations is the accepted air value equal to 295.5 the above mentioned phenomena are attributable most often to the Ar isotope composition un-equilibration in associated mineral components of the rock — some components (especially low-K mineral phenocrysts) may have an initial $^{40}Ar/^{36}Ar$ isotope ratio higher than 295.5, indicating an excess radiogenic argon presence. The geological mechanisms of this phenomenon are related to the earlier phenocryst crystallization in respect to rock groundmass crystallization. For argon sources with increased $^{40}Ar/^{36}Ar$ isotope ratio (>295.5) the following processes might be relevant: 1) melt inclusions in phenocrysts; 2) the argon contained in melt as gaseous component captured in lattice of crystallizing phenocrysts; 3) the argon retained in cores of phenocrysts during magma contamination by older sialic crustal material — cores of phenocrysts in this case represent remnants of assimilated crustal rocks that later played the role of phenocryst crystallization centers (Chernyshev et al. 1999, 2002, 2006). The phenomenon of excess radiogenic argon is characteristic especially for phenocrysts with low potassium content — pyroxene, plagioclase and amphibole. Its effect in the case of potassium-rich biotite is questionable for Miocene rocks. If different ages are obtained for biotite–groundmass pairs an effect of radiogenic argon loss of one of the fractions due to reheating or secondary processes is a more probable cause. Biotite, as well as groundmass K-feldspars and glass, are sensitive to these processes. In such a case the higher age of the pair is considered as the more dependable one.

The data set forth here and the above considerations give us a basis for concluding that volcanic rock groundmass, that evolved from erupted and consequently mostly out-gassed material, represents the most acceptable K-Ar geochronometer with the exception of samples affected by rejuvenation. Its usage for geochronological studies of young volcanic rock does not exclude a parallel, more detailed study involving also K-Ar measurements of phenocrysts. In this respect we believe, that such a detailed study as performed on volcanic rocks of the Štiavnica Stratovolcano also brings methodological benefits (Appendix 1). Out of 9 rocks studied with data on both, plagioclase phenocrysts and groundmass, in 3 cases K-Ar age values obtained from plagioclase phenocrysts and groundmass of the same rock are consistent within the analytical error intervals. However, in the case of 6 rocks (GK-110, GP-11/02, GK-16, GP-57, GK-105, GK-21) the K-Ar ages obtained from groundmass and plagioclase phenocrysts differ significantly by 1.6 to 3.3 Ma, the age values of plagioclase phenocrysts being older than the age values of groundmass in the same rock. It follows that a whole-rock sample K-Ar dating of the Štiavnica Stratovolcano rocks generally could lead to acquisition of incorrect age data. The discussed phenomenon is one of the causes of many discrepancies and contradictions among age estimations based previously upon K-Ar dating of whole-rock samples (Konečný et al. 1969; Bagdasarjan et al. 1970; Merlitsh & Spitkovskaya in Štohl 1976; Bagdasarjan in Konečný et al. 1983; Kantor et al. 1988). Another cause could be connected with the significant (±2–3 Ma) errors of earlier results due to the limitations of analytical isotope techniques more than 30 years ago. The third cause is related to a possible partial or complete rejuvenation of minerals with low closing temperature due to reheating by an extensive hydrothermal system in the central zone of the stratovolcano.

To eliminate a possible influence of excess radiogenic argon in phenocrysts of plagioclase, pyroxenes and amphiboles upon the age of dated rocks the present work is based especially upon the K-Ar dating results obtained by analyses of groundmass (matrix, glass) separated from phenocrysts. Some andesites, out of studied ones, contain subordinate biotite phenocrysts in sufficient quantity to enable Rb-Sr analyses. The Rb-Sr method of dating was applied to intrusive rocks as well as to felsic volcanic rocks of the Štiavnica Stratovolcano.

The results of Rb-Sr isochrone dating require few comments. The $^{87}Rb/^{86}Sr$ of biotites is an order of magnitude higher than the $^{87}Rb/^{86}Sr$ of other phases. In such a case it is especially biotite that determines the isochrone slope and the isochrone age is more or less the biotite age. With the exception of two samples, the MSWD parameter is greater than 1. This suggests that a geochemical dispersion of the data relatively to the isochrone regression line exists beside an analytical scatter of data points. Such a situation appears to be bound to young magmatic rocks, including rocks of the Štiavnica Stratovolcano. At low radiogenic ^{87}Sr content, inherent to such young rocks, the initial $^{87}Sr/^{86}Sr$ ratio variations affect remarkably the data point position in respect of the isochrone regression line as well as the MSWD isochrone parameter value. This effect is manifested in Rb-Sr data for rocks of the Štiavnica Stratovolcano in an unconformable position of data points representing fractions with high common Sr content (hundreds ppm) close to the $^{87}Sr/^{86}Sr$ coordinate (Fig. A in Appendix 2). The same data points determine the I_0 isochrone parameter value. As demonstrated in the Appendix 2 this parameter varies significantly between 0.7053 and 0.7085 reflecting the Sr isotope heterogeneity of the rocks studied.

New K-Ar and Rb-Sr data

The set of studied samples represents main structural units (evolutionary stages) of the Štiavnica Stratovolcano that are recognized on the 1 : 50,000 map (Konečný et al. 1998). Sampling localities are marked in the structural scheme of the stratovolcano (Fig. 2). Their geographical and geological positions are provided in electronic Appendix 3, whereas short petrographic description and chemical characteristics of analysed samples are given in Appendices 3 and 4, respectively (available only in the electronic version). Appendices 1 and 2 include the obtained K-Ar and Rb-Sr ages along with source analytical data and their individual errors.

The chemical compositions of the Štiavnica Stratovolcano samples that were used for isotope dating are given in Appen-

Table 1: Summary of reliable K-Ar and Rb-Sr isotope geochronological data for rocks of the Štiavnica Stratovolcano.

No.	Sample	Rock type	Volcanic form	Formation Complex	K-Ar age (Ma)	Rb-Sr age (Ma)
Volcanic formations pre-dating Štiavnica Stratovolcano						
1	GP-4	Pyroxene-amphibole andesite with garnet	Extrusive dome	Neresnica Formation	15.0 ± 0.4	
Lower structural unit (1st stage)						
3	GK-111	Amphibole-pyroxene andesite	Lava flow	Sebechleby Formation	14.8 ± 0.3	
4	GK-110	Amphibole-pyroxene andesite	Fragment in lahar breccia	Sebechleby Formation	14.0 ± 0.4	
5	St-6/06	Amphibole-pyroxene andesite	Lava flow	Sebechleby Formation	14.0 ± 0.4	
6	St-4/06	Pyroxene andesite matrix	Welded tuff/breccia	Lower structural unit	13.8 ± 0.4	
7	St-5/06	Pyroxene andesite fragment	Welded tuff/breccia	Lower structural unit	13.8 ± 0.4	
8	GK-107	Pyroxene andesite	Lava flow	Žibritov Complex	14.1 ± 0.3	
9	GK-106	Pyroxene andesite	Lava flow	Žibritov Complex	13.8 ± 0.4 13.7 ± 0.3	
10	GP-13	Pyroxene andesite	Lava flow	Žibritov Complex	13.4 ± 0.4	
11	St-7/06	Pyroxene andesite	Lava flow	Lower structural unit	13.5 ± 0.3	
12	St-14/06	Pyroxene andesite	Lava flow	Lower structural unit	13.5 ± 0.4	
13	GK-57	Pyroxene andesite	Lava flow	Lower structural unit	13.2 ± 0.4	
14	GP-11	Pyroxene andesite	Lava flow	Lower structural unit	13.1 ± 0.4	
Subvolcanic/intravolcanic intrusive complexes (2nd stage)						
15	St-5/99	Granodiorite	Bell-jar type pluton	Hodr.-Štiavn. Intr. Complex		13.4 ± 0.2
16	St-2/04	Granodiorite	Bell-jar type pluton	Hodr.-Štiavn. Intr. Complex		13.3 ± 0.6
17	St-4/08	Diorite	Bell-jar type pluton	Hodr.-Štiavn. Intr. Complex		13.3 ± 0.2
Middle structural unit (caldera filling, 3rd stage)						
18	St-83/91*	Biotite-amphibole andesite	Extrusive dome	Studenec Formation	12.7 ± 0.4*	12.4 ± 0.1
19	GK-100	Pyroxene-biotite-amphibole andesite	Lava flow	Studenec Formation	13.1 ± 0.3	
20	GK-16	Biotite-amphibole andesite	Extrusive dome	Studenec Formation	12.8 ± 0.3	12.9 ± 0.5
21	GK-20	Pyroxene-biotite-amphibole andesite	Extrusive dome	Studenec Formation	13.0 ± 0.4	12.4 ± 0.6
Upper structural unit (4th stage)						
22	St-9/06	Pyroxene andesite	Lava flow	Baďan Formation	12.6 ± 0.3	
23	St-10/06	Pyroxene andesite	Lava flow	Baďan Formation	12.5 ± 0.3	
24	GK-105	Biotite-amphibole-pyroxene andesite	Lava flow	Sitno Effusive Complex	12.7 ± 0.3	12.3 ± 0.2
25	KSD-2	Biotite-amphibole-pyroxene ignimbrite	Welded tuff	Drastvica Formation		12.0 ± 0.2
26	St-1/06	Pyroxene andesite	Lava flow	Breznica Complex	12.9 ± 0.3	
27	St-11/06	Pyroxene andesite ± biotite	Lava flow	Priesil Formation	13.0 ± 0.3	
28	St-12/06	Amphibole-pyroxene andesite ± biotite	Lava flow	Priesil Formation	12.4 ± 0.3	12.3 ± 0.7
29	St-15/06	Pyroxene andesite	Lava flow	Inovec Formation	12.2 ± 0.3	
30	St-16/06	Amphibole-pyroxene andesite	Lava flow	Žiar Complex	12.0 ± 0.3	
Rhyolites of the Jastrabá Formation (5th stage)						
31	St-18/06	Rhyolite	Dyke	Jastrabá Formation		12.2 ± 0.8
32	GK-21	Rhyolite	Dyke	Jastrabá Formation	12.2 ± 0.3 11.9 ± 0.3	
33	KSD-1	Rhyolite (K-metasomatism)	Extrusive dome	Jastrabá Formation	11.5 ± 0.3	
34	V-7/91c*	Rhyolite (K-metasomatism)	Extrusive dome	Jastrabá Formation	11.6 ± 0.3*	
35	L-8/91*	Rhyolite (perlite)	Fragment in extr. breccia	Jastrabá Formation	11.4 ± 0.4*	12.1 ± 0.1
36	St-6/08B	Rhyolite (perlite)	Fragment in extr. breccia	Jastrabá Formation		11.8 ± 0.1
37	Kl-1/91*	Rhyolite	Dyke	Jastrabá Formation	11.4 ± 0.3*	
Post-rhyolite volcanic formations — alkali basalts						
38	St-84/91*	Nepheline basanite	Lava neck		7.8 ± 0.4*	
39	St-85/91B*	Nepheline basanite	Lava neck		5.7 ± 0.4*	
40	S-B3/02	Nepheline basanite	Lava flow		0.45 ± 0.03	
41	S-B7/02	Nepheline basanite	Lava neck		0.42 ± 0.03	
42	S-B8/02	Nepheline basanite	Lava flow		0.43 ± 0.03	

* — data published already by Chernyshev et al. (1995). Numbers 1–42 correspond to sample numbers on the structural scheme (Fig. 2).

dix 4 along with a short commentary. The data as shown in the diagram $Na_2O+K_2O-SiO_2$ (Fig. B in electronic Appendix 4) are comparable to earlier results obtained from volcanic rocks of the Central Slovakia Volcanic Field (Konečný at al. 1995). Their composition is close to high-potassium rocks of andesite-dacite suites in volcanic belts of the developed island arcs or continental margins (Lexa & Konečný 1998).

Appendix 1 presents all new K-Ar data. It also demonstrates the relationship among the K-Ar ages of groundmass, plagioclase and/or biotite separated from common samples. Results that are considered reliable and serve as a basis of the following discussion and conclusions, are indicated by bold type and grey background. Reliability of results has been evaluated on the basis of criteria mentioned in the part on methodology and compatibility with other results. Comments on the selection of reliable results in the case of individual samples are given below. Appendix 2 presents the results of Rb-Sr isochron dating, whereas Table 1 presents reliable results of K-Ar and Rb-Sr dating as accepted age values with 2 σ errors. Here we have also included results published by Chernyshev et al. (1995) as they were not discussed yet in the context of other data and the evolution of the Štiavnica Stratovolcano.

The primary objective of the Rb-Sr isochrone dating application in the present work was dating of intrusive rocks in the area of younger hydrothermal system overprint (regional propylitic alteration associated with the extensive system of epithermal veins) as the closure temperature of the Rb-Sr system rock-forming minerals (biotite, feldspars) is higher than for the K-Ar system. This is an important feature of the Rb-Sr system if we take into account that the younger hydrothermal system has reached temperatures of 250–300 °C (Kovalenker et al. 1991; Onačila et al. 1995). Moreover, Rb-Sr age data represent the independent information that can be used to control results of K-Ar dating. Such a possibility has been used in the case of rocks containing biotite. In so doing 3–5 mineral fractions separated from a common rock were analysed. In two cases (samples GK-105, L-8/91) Rb-Sr measurements were limited to analyses of pairs biotite–whole rock, or biotite–glass. Out of 6 samples studied by both methods 4 andesite samples show a concordant K-Ar and Rb-Sr isochron ages that agree within the 2 σ error intervals while two felsic rock samples (L-8/91 rhyolite, GK-21 rhyodacite) exhibit a differences between the K-Ar ages and Rb-Sr ages that exceed the error intervals as much as 1.5–2 times.

Comments on the reliability of individual results

Most of the results of K-Ar dating obtained from groundmass fraction and Rb-Sr isochrone dating are reliable and need no comments. However, some of the results are contradictory and require comments on how reliable results have been chosen.

No. 1 (sample GP-4): The obtained K-Ar isotope age of 15.0 ± 0.4 Ma on groundmass fraction corresponds to Early Badenian. That is in agreement with the structural position below the base of the Štiavnica Stratovolcano. The apparent age of 14.6 ± 0.4 Ma from plagioclase phenocrysts overlaps with results from the overlying rocks, so it is not considered representative.

No. 2 (sample GK-2/01): The sample represents a lava flow filling a paleovalley eroded in rocks of the *Sebechleby Formation*. However, the age of 15.2 ± 0.4 Ma obtained from pyroxene andesite groundmass is older if compared with ages of the underlying formation in the range 14.8 ± 0.3 to 14.0 ± 0.4 Ma (Appendix 1 and Table 1).

No. 4 (sample GK-110): K-Ar dating of groundmass fraction has provided the reliable age 14.0 ± 0.4 Ma. The result 15.6 ± 0.5 Ma from plagioclase phenocrysts is not considered representative, probably due to excess radiogenic argon.

No. 9 (sample GK-106): K-Ar dating of groundmass fraction has provided the age 13.7 ± 0.3 Ma. In this case plagioclase phenocrysts have provided a compatible result 13.8 ± 0.4 Ma.

Nos. 12 and 13 (samples St-14/06 and GK-57): Results of K-Ar dating of groundmass fractions 13.5 ± 0.3 and 13.2 ± 0.4 place these lava flows into the upper parts of the lower structural unit (first stage). The result 15.1 ± 0.7 Ma from plagioclase phenocrysts of the sample No. 13 is not considered representative, probably due to excess radiogenic argon.

No. 14 (sample GP-11): K-Ar dating on groundmass fraction has provided the age 13.1 ± 0.4 Ma. The result 11.8 ± 0.5 Ma obtained from plagioclase phenocrysts is not considered representative.

No. 17a (sample St-2/08): An attempt to date the dyke by Rb-Sr isochrone method has not been successful (Fig. A in Appendix 2). Analyses of individual fractions do not fall on a well-defined isochrone. The upper and lower limits for the age are 16 and 11 Ma.

No. 18 (sample St-83/91): K-Ar dating of mineral fractions provided the following ages: plagioclase — 15.8 ± 2.0 Ma, amphibole — 14.8 ± 1.2 Ma and biotite — 12.7 ± 0.4 Ma; K-Ar isochrone provided the age 12.4 ± 0.2 Ma; Rb-Sr isochrone dating provided the age 12.4 ± 0.1 Ma. Both, K-Ar and Rb-Sr isochrone ages overlap with data from overlying andesites of the upper structural unit. As the K-Ar isochrone is affected by excess argon in plagioclase and amphibole the K-Ar age of biotite is considered the most representative.

No. 20 (sample GK-16): K-Ar dating provided the age 11.8 ± 0.3 Ma from groundmass fraction and 12.8 ± 0.3 Ma on biotite fraction; the result 15.1 ± 0.5 Ma obtained from plagioclase phenocrysts reflects excess radiogenic argon. Rb-Sr isochrone dating (Fig. A in Appendix 2) provided the age 12.9 ± 0.5 Ma. In this case we assume that groundmass has been affected by radiogenic argon loss (due to unrecognized alteration?). It follows that the K-Ar age for the biotite fraction and Rb-Sr isochrone age are considered representative.

No. 21 (sample GK-20): K-Ar dating provided the age 11.8 ± 0.3 Ma from the groundmass fraction and 12.1 ± 0.3 Ma from the biotite fraction. The plagioclase fraction provided the result 13.0 ± 0.4 Ma. Rb-Sr isochrone dating pointed to the age 12.4 ± 0.6 Ma. Usually the Rb-Sr isochrone age is considered the most reliable one and plagioclase apparent K-Ar ages are affected by the excess argon phenomena. However, in this case only the K-Ar age on plagioclase fits the geological position. Other results are too young considering the ages of overlying andesites of the upper structural unit.

No. 24 (sample GK-105): K-Ar dating of groundmass fraction provided the age 12.7 ± 0.3 Ma that is within the error limits from the Rb-Sr isochron age 12.3±0.2 Ma. The result 15.4±0.6 Ma from plagioclase phenocrysts is not considered representative, most probably due to excess radiogenic argon.

No. 28 (sample St-12/06): K-Ar dating of groundmass fraction provided the age 12.4±0.3 Ma that is within the error limits from the Rb-Sr isochron age 12.3±0.7 Ma.

No. 32 (sample GK-21): K-Ar dating of groundmass provided the age 11.9±0.3 Ma, the biotite fraction produced the age 12.2±0.3 Ma, and the plagioclase fraction 13.7±0.4 Ma perhaps reflecting excess radiogenic argon. Rb-Sr isochron dating provided the age 10.5±0.2 Ma. The K-Ar ages of the groundmass and biotite fraction are considered the most reliable ones.

No. 35 (sample L-8/91): K-Ar dating of biotite and glass provided the ages 12.7±0.4 Ma and 11.4±0.4 Ma respectively. The Rb-Sr isochron dating provided the age 12.1±0.1 Ma. The result obtained on biotite overlaps with ages of older andesites. Perlite glass is sensitive to possible radiogenic argon loss. The Rb-Sr isochron age is considered the most representative.

Discussion – evolution of the Štiavnica Stratovolcano

Volcanic formations preceding the Štiavnica Stratovolcano

Biostratigraphic dating of associated sedimentary and volcano-sedimentary rocks suggests the Early Badenian age (Zone NN5) for volcanic activity of garnet-bearing andesites (Kantorová 1962; Čechovič & Vass 1962; Lehotayová 1962; Lehotayová in Vass et al. 1979; Konečný et al. 1983; Kováč et al. 2005). The same age is applicable for the early volcanic activity of garnet-bearing andesites/dacites in the Börzsöny mountain range, located further southward (Karátson et al. 2000). According to Kováč et al. (2005) sedimentary rocks of the lowermost Badenian corresponding to the nannoplankton Zone NN4 are missing in the Slovak territory. The Early Badenian transgression reached the territory early during the NN5 Zone (<15.5 Ma), or early during the planktonic foraminiferal Zone *Orbulina suturalis* (<15.1 Ma). K-Ar dating of garnet-bearing andesite from the locality Breziny south of Zvolen (No. 1) to **15.0±0.4 Ma** fits well the biostratigraphic data. Older results of isotope dating of garnet-bearing andesites in the range 16.2±0.2 Ma to 15.7±1.4 Ma (Bagdasarjan in Konečný et al. 1969; Repčok 1978, 1981) are either erroneous or they imply volcanic activity before the Early Badenian transgression. Equivalent garnet-bearing andesites of the Börzsöny mountain range in Hungary show K-Ar ages in the interval 16.0–14.5 Ma (Karátson et al. 2000). Apparently, garnet-bearing andesites represent a longer lasting volcanic activity. A partial overlap with volcanic activity of the first stage of the Štiavnica Stratovolcano (the oldest reliable age obtained is 14.8±0.3 Ma) cannot be excluded on the basis of available data. We consider **14.8 Ma** as a probable upper limit on their age in the area of the Štiavnica Stratovolcano.

Lower structural unit (1st stage) of the Štiavnica Stratovolcano

Previous dating of the 1st stage rocks by the FT method provided ages in the interval 16.5±0.5 Ma to 15.9±0.8 Ma (Repčok 1980, 1981, 1984). New dating has provided a set of reliable results in the interval **14.8±0.3 Ma** to **13.1±0.4 Ma**, with most results in the interval **14.0±0.4 Ma** to **13.5±0.3 Ma** (Table 1).

The *Sebechleby Formation* in the southern sector of the stratovolcano represents a relatively older lithostratigraphic unit of the 1st stage (Konečný et al. 1998). Relationship of the formation to biostratigraphically dated volcano-sedimentary rocks in the boreholes GK-3 Rykynčice (Lehotayová in Konečný et al. 1966; Brestenská et al. 1980; Planderová in Konečný et al. 1983) and ŠV-8 Dolné Semerovce (Vass et al. 1981; Ozdínová 2008) points to the middle(?) to late Early Badenian age of the formation. The results of new dating in the range **14.8±0.3 Ma** to **13.8±0.4 Ma** (Nos. 3–7) are compatible with such a biostratigraphic assignment. The result **15.2±0.4 Ma** (No. 2) would be compatible with biostratigraphic assignment of the formation as well as with the isotope age of underlying volcanic products of garnet-bearing andesites (see above) only in the case that the real age is close to the lower limit of the error interval. This lava flow is also relatively younger as it fills a paleovalley in older rocks of the formation. Because of incompatibility with younger ages on underlying rocks it is not considered reliable. Taking into account the reliable results (Table 1), the biostratigraphic evidence and a possible overlap of the 1st stage with activity of garnet-bearing andesites, **15.0 Ma** seems to be the best choice for the lower limit of the 1st stage volcanic activity. However, volcanic activity of the 1st stage has not started at the same time in all sectors of the stratovolcano. In the SW sector of the stratovolcano rocks of the 1st stage rest on uppermost Lower Badenian marine sedimentary rocks (Brestenská in Karolus et al. 1975). Considering correlation of chronostratigraphic units with the time scale (Kováč et al. 2005; Harzhauser & Piller 2007) volcanic activity of the 1st stage started here as late as 14.0 to 13.6 Ma. That correlates with the absence of the *Sebechleby Formation* in this sector of the stratovolcano (Konečný et al. 1998).

The *Žibritov Effusive Complex* in the south-eastern sector of the stratovolcano represents a relatively younger lithostratigraphic unit of the 1st stage overlying the *Sebechleby Formation* (Konečný et al. 1998). There is no biostratigraphic evidence available. New isotope dating has provided 4 results (Nos. 8–11) in the interval **14.1±0.8 Ma** to **13.4±0.6 Ma** (Table 6) around the Early/Late Badenian boundary. The lava flow at the locality Ficberg (No. 11) has formerly been assigned to the upper structural unit (4th stage) of the stratovolcano on the basis of erroneous K-Ar dating to 11.4±0.3 Ma (Bagdasarjan et al. 1970).

New results of isotope dating of two pyroxene andesite lava flows next to Machulince in the western sector of the stratovolcano, namely **13.5±0.3 Ma** and **13.2±0.4 Ma**, respectively, assign these lava flows to the youngest products of the 1st stage of the stratovolcano, corresponding to the Late Badenian. However, on the basis of geological mapping these lava flows have formerly been assigned to the upper structural unit (4th stage) (Konečný et al. 1998) and their real assignment should be further clarified by detailed field investigation. Pyroxene-rich sandy deposits in the interval 194–230 m of the borehole ŠV-8 Dolné Semerovce assigned to the lowermost

Upper Badenian (Vass et al. 1981; Ozdínová 2008) may represent a volcano-sedimentary equivalent.

K-Ar dating of the 1st stage pyroxene andesite lava flow south of Nová Baňa (No. 14) provided the age of **13.1 ± 0.4 Ma**. As the lava flow is relatively close to the Nová Baňa epithermal system and shows signs of weak hydrothermal alteration its relatively young age might be a result of partial rejuvenation.

The upper limit for the time interval of the 1st stage of the stratovolcano is set forth by (1) the Late Badenian age of overlying sedimentary rocks in the borehole ŠV-8 Dolné Semerovce (see below) and (2) by results of isotope dating of rocks from the *Hodruša-Štiavnica Intrusive Complex* (Nos. 15–17) in the range 13.4 ± 0.2 Ma to 13.3 ± 0.2 Ma. The intrusive complex is younger than rocks of the 1st stage (Konečný et al. 1998; Konečný & Lexa 2001). It follows that the most probable interval of the 1st stage volcanic activity of the Štiavnica Stratovolcano is **15.0–13.5 Ma** (middle Early Badenian to early Late Badenian).

Denudation and emplacement of subvolcanic intrusive complexes (2nd stage)

Biostratigraphic evidence points to a Late Badenian age (Zone NN6) for sedimentary rocks corresponding to the denudation of the 1st stage stratovolcano (Vass et al. 1981; Ozdínová 2008) and to a late Late Badenian age for lacustrine sediments related to the early caldera subsidence (Planderová in Konečný et al. 1983).

Previous attempts to date rocks of subvolcanic intrusive complexes by the K-Ar method on whole-rock samples (Bagdasarjan et al. 1970; Merlitsh & Spitkovskaya in Štohl 1976; Konečný et al. 1983) and by the FT method on mineral fractions (Repčok 1981, 1984) failed due to extreme scatter (19.5 ± 0.8 to 10.5 ± 0.5 Ma) and contradiction between individual results reflecting variably contamination by Hercynian basement rocks, excess radiogenic argon in low-K phases and/or rejuvenation. Discordant ages obtained from amphiboles and biotites (Repčok 1981, 1984) imply resetting of biotite ages. Only single K-Ar dating of the biotite mineral fraction provided a reasonable result of 13.9 ± 0.1 Ma (Kantor et al. 1988).

The most reliable results obtained in the present work come from samples of the *Hodruša-Štiavnica Intrusive Complex*. Isotope dating of granodiorite pluton at two localities (Nos. 15–16) by the Rb-Sr method provided very close ages of **13.4 ± 0.2 Ma** and **13.3 ± 0.6 Ma**. Dating of diorite intrusion provided the same age **13.3 ± 0.2 Ma**. These results assign the *Hodruša-Štiavnica Intrusive Complex* to the Late Badenian as assumed on the basis of geological data (Konečný et al. 1998; Konečný & Lexa 2001).

Dating of granodiorite to quartz-diorite porphyry stocks and dyke clusters of the *Zlatno* and *Tatiar Intrusive Complexes* has not been successful. Attempts to date these rocks failed because of alterations of related porphyry hydrothermal systems and possible rejuvenation by younger epithermal systems. K-Ar dating of granodiorite porphyry from the locality Šementlov by Chernyshev et al. (1995) to **11.4 ± 1.2 Ma** serves as an example. An attempt to date the granodiorite porphyry

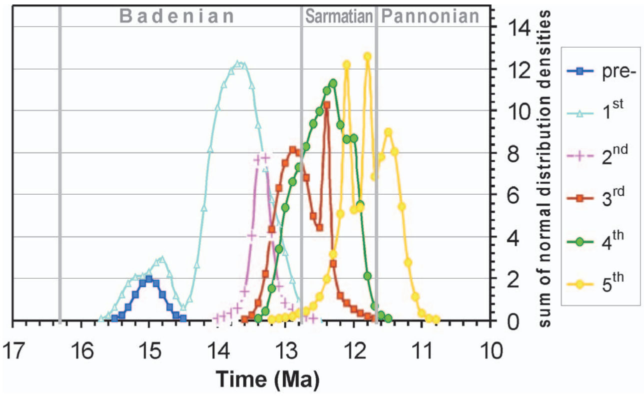

Fig. 6. Sums of radiometric age normal distribution densities for evolutionary stages of the Štiavnica Stratovolcano based on K-Ar and Rb-Sr ages presented in Table 1. The curves for individual stages reflect the number of individual results, values of individual results and their errors. In that way they summarize results of individual stages and allow for their mutual comparison.

intrusion at the locality Zlatno by the Rb-Sr method (Kráľ et al. 2002) has failed too. The rock, including mafic enclaves up to 0.5 m in diameter, was isotopically homogenized at subsolidus temperatures. Results from separated amphiboles and biotites imply, that amphibole was enriched in radiogenic Sr lost by biotite during a younger event. The biotite–whole-rock isochron gave the apparent age **10.6 Ma**.

The same applies to the younger *Banisko Intrusive Complex*. Owing to regional alteration related to thermal anomaly of extensive system of epithermal veins no reliable results have been obtained. FT dating of a quartz-diorite sill close to the locality Zlatno has provided apparent ages for amphibole and biotite of 13.4 ± 0.6 Ma and 13.6 ± 0.8 Ma respectively (Repčok 1984). As some of the sills of the complex intruded into the lowermost parts of the Štiavnica Caldera filling (Figs. 3, 5) the age of the caldera filling (13.1–12.7 Ma) also represents the upper limit for the age of the intrusive complex (compare Fig. 6). The value 12.9 Ma in the middle of this interval is considered the most probable upper limit. It follows that the subvolcanic intrusive complexes of the Štiavnica Stratovolcano were emplaced in the time interval **13.4–12.9 Ma**, corresponding to the Late Badenian.

Middle structural unit (caldera filling, 3rd stage)

Palynomorphs in sediments interbedded with rocks of the *Studenec Formation* within the caldera as well as at the outskirts of the stratovolcano point to the interval late Late Badenian to Early Sarmatian (Planderová in Konečný et al. 1983). Overlying sediments have been assigned to the Lower Sarmatian (Sitár 1973; Planderová in Konečný et al. 1983).

Previous isotope dating by the K-Ar and FT methods provided erroneous ages in the interval 16.4–14.8 Ma (Konečný et al. 1969; Repčok 1978–1981). New isotope dating by both, K-Ar and Rb-Sr methods, provided reliable ages in the interval **13.1 ± 0.3 Ma** to **12.4 ± 0.1 Ma** (see discussion to individual samples above and Table 1) that are in agreement with biostratigraphic evidence. However, the youngest data are not compatible with ages on some of the overlying rocks of the upper structural level (4th stage) (see bellow). Considering the mutual overlap of apparent ages of the 3rd and 4th stages (Fig. 6) the best choice for the upper limit of the 3rd stage and lower limit of the 4th stage is **12.7 Ma**. Considering correlation of chronostratigraphic units with the time scale (Kováč et al. 2005; Harzhauser & Piller 2007), the volcanic activity of the 3rd stage took place during the late Late Badenian and despite the palynological evidence probably did not extend into the Early Sarmatian.

Upper structural unit (4th stage)

Biostratigraphic data from marine sediments interbedded with rocks of the upper structural unit in the SW sector of the stratovolcano reveal the Early Sarmatian age (Brestenská 1970; Karolus & Váňová 1973). Freshwater lacustrine deposits interbedded with volcanic formations of the fourth stage elsewhere contain remnants of macroflora and palynomorphs implying the same age (Němejc 1967; Sitár 1973; Planderová in Konečný et al. 1983). However, Kováč et al. (2005) questioned the ability to distinguish Early and Late Sarmatian.

The upper structural unit comprises a succession of poorly correlated volcanic formations and complexes post-dating the Štiavnica Caldera and pre-dating rhyolite volcanism of the 5th stage. Fig. 5 shows their probable succession. Previous isotope dating by the K-Ar and FT methods provided mostly erroneous ages in the interval 15.0–9.9 Ma (Konečný et al. 1969; Bagdasarjan et al. 1970; Repčok 1978, 1981). New isotope dating of the 4th stage rocks (Nos. 22–30, Table 1) by K-Ar as well as Rb-Sr methods provided ages in the interval **13.0 ± 0.3 Ma** to **12.0 ± 0.2 Ma**. We have already discussed above that the probable lower limit on the age of the 4th stage rocks is **12.7 Ma**. The upper limit is constrained to **12.2 Ma** by the overlap with results obtained from younger rhyolites (Table 1, Fig. 6) and by ages of rhyolites in the Nová Baňa area in the interval 12.31 ± 0.44–12.03 ± 0.38 Ma (Lexa & Pécskay 2010). Considering correlation of chronostratigraphic units with the time scale (Kováč et al. 2005; Harzhauser & Piller 2007), the volcanic activity of the 4th stage took place during Early Sarmatian.

Rhyolites of the Jastrabá Formation (5th stage)

Rhyolite activity accompanied the resurgent horst uplift and contemporaneous subsidence of the Žiar Depression. Palynological evidence points to the Late Sarmatian to Early Pannonian age (Planderová in Konečný et al. 1983).

With few exceptions the results of previous isotope dating by the K-Ar and FT methods fall in the interval 12.9–10.7 Ma (Konečný et al. 1969; Bagdasarjan et al. 1970; Bojko et al. in Štohl 1976; Merlitsh & Spitkovskaya in Štohl 1976; Repčok 1981, 1982). The results of new dating by K-Ar, as well as Rb-Sr methods (Nos. 31–37, Table 1) fall in the interval **12.2 ± 0.8 Ma** to **11.4 ± 0.4 Ma**. This interval is comparable with the results of K-Ar dating of the Jastrabá Formation rhyolites in the Nová Baňa area and Kremnické vrchy mountain range that fall into the intervals 12.3 ± 0.4–12.0 ± 0.4 Ma and 12.3 ± 0.4–11.5 ± 0.4 Ma, respectively (Lexa & Pécskay 2010). Considering correlation of chronostratigraphic units with the time scale (Kováč et al. 2005; Harzhauser & Piller 2007), the rhyolite volcanic activity of the Jastrabá Formation (5th stage) took place during the Late Sarmatian to earliest Pannonian time.

Post-rhyolite volcanic formations — high alumina basalts

The volcanic activity of high alumina basalts and basaltic andesites of the *Šibeničný vrch Complex* post-dated rhyolite volcanites of the *Jastrabá Formation* in the Žiar Depression. The reported K-Ar ages fall in the range **11.1 ± 0.8** to **8.2 ± 0.5 Ma** (Balogh et al. 1998), that corresponds to the Early to Late Pannonian time. New data are not available.

Post-rhyolite volcanic formations — alkali basalts

K-Ar dating of alkali basalt necks at Kysihýbel (No. 38) and Banská Štiavnica (No. 39) on whole-rock samples provided results of **7.8 ± 0.4 Ma** and **5.7 ± 0.4 Ma**, respectively. While the first result is compatible with the result of previous dating (7.31 ± 0.24 Ma, Konečný et al. 1999) the second result seems to be erroneous as previous dating provided results of 7.24 ± 0.25 Ma (Konečný et al. 1999) and 7.32 ± 0.23 Ma (Kantor & Wiegerová 1981). The ages of both alkali basalt necks correspond to the latest Pannonian to Pontian time.

The alkali basalt volcano Pútikov vŕšok is the youngest volcano in Slovakia. Previous K-Ar dating of its lava flow using a whole-rock sample provided an age of 0.53 ± 0.16 Ma (Balogh et al. 1981). Superposition over the Hron river Riss terrace points to age in the interval 0.15–0.12 Ma (Šimon & Halouzka 1996), while optically stimulated luminescence (OSL) dating of underlying sediments provided an age of 102 ± 11 ka (Šimon & Maglay 2005). New K-Ar dating of groundmass fractions carried out on 3 samples from different parts of the volcano provided very consistent results of **0.45 ± 0.06 Ma**, **0.42 ± 0.06 Ma** and **0.43 ± 0.06 Ma**, respectively. It follows that the younger ages reported by Šimon & Halouzka (1996) and Šimon & Maglay (2005) obtained by indirect methods are questionable.

Ages of mineralization types

The high sulphidation system of Šobov is a part of the magmatic-hydrothermal system driven by diorite intrusion (Onačila et al. 1995; Lexa et al. 1999a,b). Such systems are almost contemporaneous with emplacement of the parental intrusion (Sillitoe 2010). The Rb-Sr isochron age of diorite 13.3 ± 0.2 Ma (Table 1) represents the best estimate of the mineralization age. The same type of argument is also applicable for the magnetite skarn and intrusion-related stockwork/disseminated base metal mineralizations with granodiorite as the parental intrusion (Onačila et al. 1995; Koděra et al. 1998, 2004; Lexa et al. 1999a). Their age is approximated by Rb-Sr isochron ages of granodiorite 13.4 ± 0.2 and 13.3 ± 0.6 Ma. However, considering the relative ages of diorite and granodiorite intrusions, these mineralizations are relatively younger than the Šobov high sulphidation system. We have no K-Ar data for the porphyry/skarn Cu ± Au, Mo mineraliza-

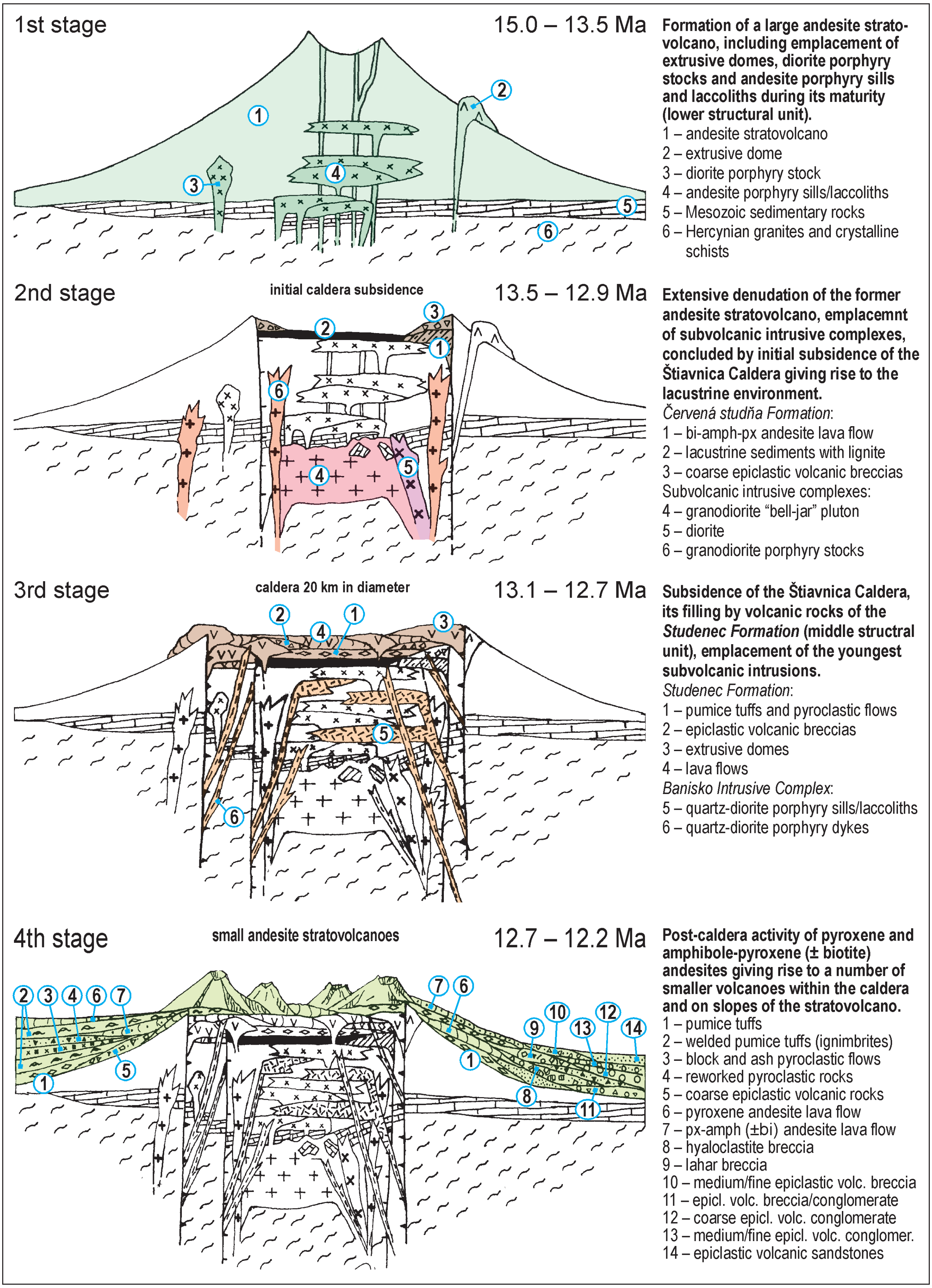

Fig. 7. Evolution of the Štiavnica Stratovolcano. Modified after Konečný & Lexa 2001. *Continued on the next page.*

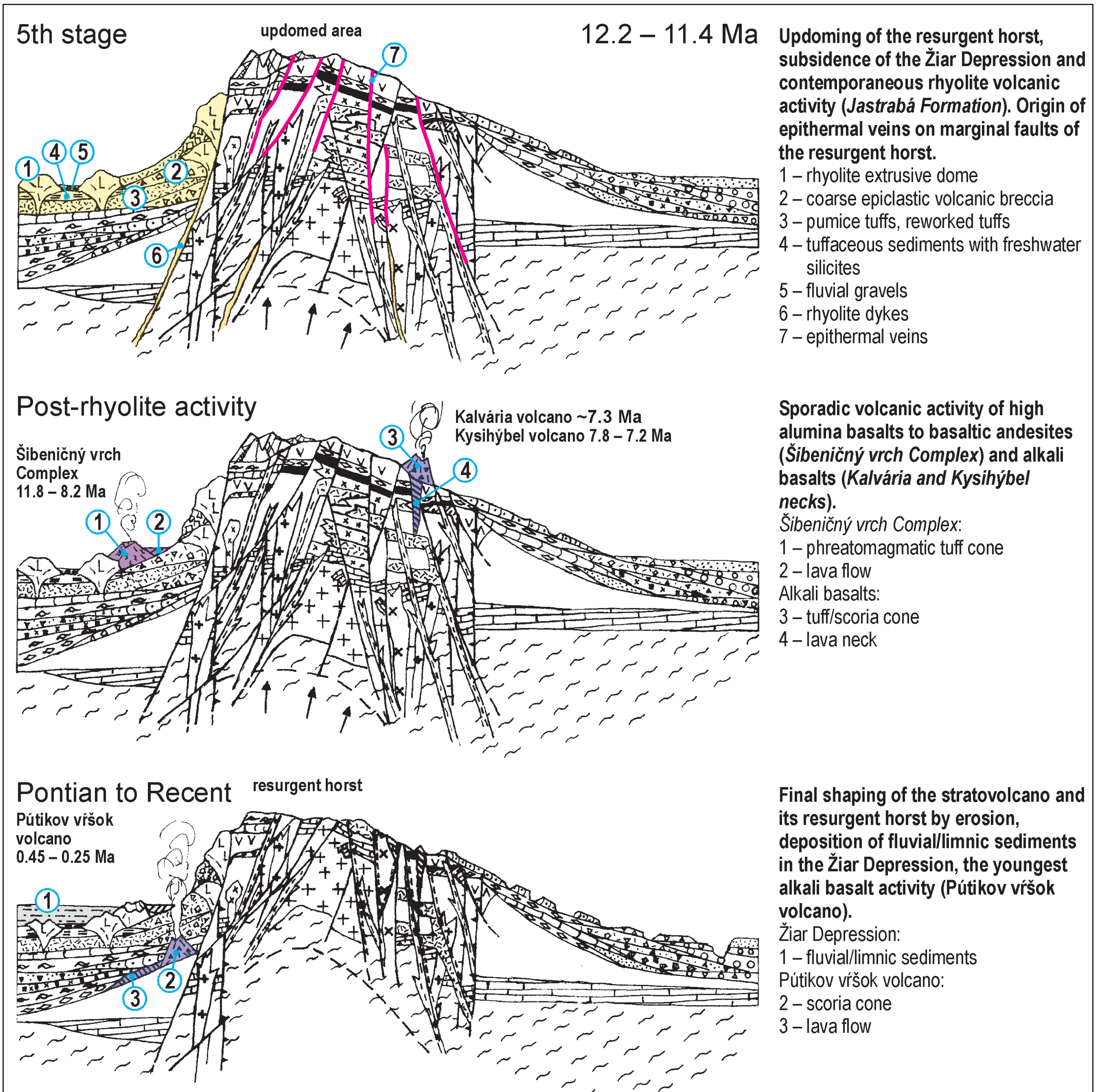

Fig. 7. *Continued from the previous page.*

tion related to the emplacement of granodiorite porphyry stocks and dyke clusters (Onačila et al. 1995; Lexa et al. 1999a) and an attempt to apply Rb-Sr isochron method has not been successful due to rejuvenation (Kráľ et al. 2002). Parental intrusions of granodiorite porphyry cross-cut granodiorite and are cross-cut by quartz-diorite porphyry dykes of the *Banisko Intrusive Complex*. This geological position places their origin into the time interval 13.1 ± 0.2 Ma.

Association of the epithermal gold mineralization at the Rozália mine with the early stage of the caldera subsidence and its origin prior to the emplacement of the quartz-diorite sills of the *Banisko Intrusive Complex* (Koděra & Lexa 2003; Koděra et al. 2005) place evolution of this mineralization into the time interval 13.0 ± 0.1 Ma.

Kraus et al. (1999) dated illites from the above mentioned mineralizations. K-Ar dating of $2M_1$ type illite from Šobov provided the age 12.4 ± 0.1 Ma, of $2M_1 >> 1M$ type illite from argillites of the stockwork/disseminated base metal mineralization provided the age 11.5 ± 0.3 Ma, while $2M_1 >> 1M$ type illite from the epithermal gold mineralization at the Rozália mine provided the age 11.9 ± 0.3 Ma. Such results are in conflict with the established geological position. The Šobov high sulphidation system is cross-cut by younger base metal epithermal veins showing temperatures over 300 °C (Kovalenker et al. 1991) and the stockwork/disseminated base metal mineralization and epithermal gold mineralization extend next to the Rozália vein in the hottest Cu-zone of the younger epithermal system (Onačila et al. 1995), where temperature could reach

350 °C. A partial to complete rejuvenation due to long lasting reheating by younger epithermal system is highly probable.

The extensive system of precious/base metal low to intermediate sulphidation epithermal veins evolved during the uplift of the resurgent horst. K-Ar dating of adularia in epithermal veins provided the ages 12.0–10.7 Ma (Kantor & Ďurkovičová 1985; Kantor et al. 1988). K-Ar dating of $1M>>2M_1$ type illite from the Terézia vein at the Weiden gallery provided the age 11.4±0.2 Ma (Kraus et al. 1999). Rejuvenated ages of 11.5±0.3 Ma and 11.9±0.3 Ma also obtained from $2M_1>>1M$ type illites from older mineralizations (see above) are considered as indirect data. Dating of rhyolites to the time interval 12.2–11.4 Ma confirmed that evolution of the epithermal system took place during and after magmatic activity of the rhyolites (Kovalenker et al. 1991; Onačila et al. 1995; Chernyshev et al. 1995; Lexa et al. 1999a; Háber et al. 2001; Lexa 2001). Lexa & Pécskay (2010) confirmed the same relationship in the case of rhyolites and epithermal system in the Nová Baňa ore deposit.

Lifespan of the Štiavnica Stratovolcano and breaks in volcanic activity

The lifespan of the stratovolcano is definitely shorter than assumed earlier. While Konečný et al. (1983, 1998) assumed its evolution in the Early Badenian through Early Pannonian time (16.4–10.7 Ma), the presented results from new K-Ar and Rb-Sr isotopic dating imply that it was active in the interval **15.0–11.4 Ma** (middle Early Badenian–earliest Pannonian). The most prolonged first stage, representing construction of the compound andesite stratovolcano, took almost a half of the total duration of volcanic activity (1.5 Ma out of 3.6 Ma), whereas three later evolutionary stages representing emplacement of subvolcanic/intravolcanic intrusions, caldera subsidence and activity of post-caldera andesite volcanoes lasted only around 0.5 Ma each and the 5th stage of rhyolite activity lasted around 0.8 Ma.

The results of isotopic dating and their errors provide an illusion of continuous volcanic/magmatic activity. However, frequent unconformities and evidence for associated extensive erosion (Konečný et al. 1998; Konečný & Lexa 2001) point to frequent breaks in volcanic activity of variable duration. Analogy with recent volcanoes implies that in reality shorter periods of volcanic/magmatic activity were separated by longer lasting breaks giving opportunities for erosion. Thus several unconformities between lithostratigraphic units of the 1st stage explain its unusually long duration. A longer lasting break in volcanic activity took place between the 1st and 3rd stages — prior to initial subsidence of the caldera. During this break the former compound andesite stratovolcano with elevation 3000–4000 m had been denudated down to the level of intravolcanic intrusions and thickness 500–1000 m in the central zone. However, this break in volcanic activity only partially overlapped with a break in magmatic activity as emplacement of subvolcanic/intravolcanic intrusive complexes took place towards its end. Another significant break in volcanic activity took place following the caldera subsidence. Volcanic rocks of the 4th stage andesite volcanoes rest at many places on a levelled surface over the caldera fault. Lithostratigraphic units of the 4th stage are often separated by minor unconformities (Fig. 5) implying minor breaks in volcanic activity also during this stage. Finally, a major unconformity and related break in volcanic activity separated the rhyolites of the 5th stage from the andesites of the 4th stage.

Conclusions

We have applied the low-blank K-Ar method coupled with the Rb-Sr isochron method to a representative set of magmatic rocks that systematically cover the different structural units and evolutionary stages of the Neogene Štiavnica Stratovolcano. The K-Ar study of mineral components of common volcanic rocks has confirmed the phenomena of the excess radiogenic ^{40}Ar in plagioclase phenocrysts. Therefore, our recent geochronological study of the Štiavnica Stratovolcano was based especially upon K-Ar dating of groundmass fractions. Its combination with the Rb-Sr isochron dating provided highly reliable results.

Former attempts to date subvolcanic intrusive rocks using whole-rock samples failed owing to possible effects of contamination and partial rejuvenation due to regional hydrothermal alteration associated with the extensive systems of late stage epithermal veins overlapping with the extent of subvolcanic intrusions. We have managed to obtain reliable results for the granodiorite/diorite pluton of the *Hodruša Intrusive Complex* using the Rb-Sr isochron method.

Results of new K-Ar and Rb-Sr isotopic dating confirmed the succession of volcanic/magmatic activity based on results of geological mapping, superposition of lithostratigraphic units and major unconformities. At the same time we have achieved compatibility between the isotope and biostratigraphic ages of lithostratigraphic units by using the latest version of the geological time scale (Harzhauser & Piller 2007) and biostratigraphic assignment of sedimentary formations (Kováč et al. 2005).

On the basis of new data and critical evaluation of older evidence, we are able to assign the most probable time intervals to the established evolutionary stages of the Štiavnica Stratovolcano and volcanic formations below and above. Based on the above discussion evolution of the Štiavnica Stratovolcano can be summarized as follows (Fig. 7):

1. Volcanic activity of garnet-bearing andesites at dispersed centers took place prior to the evolution of the Štiavnica Stratovolcano in the time interval 16.0–14.8 Ma (early to middle Early Badenian). A partial overlap with volcanic activity of the lower structural unit (1st stage) cannot be excluded.

2. Evolution of the extensive compound stratovolcano of pyroxene and amphibole-pyroxene andesites took place during the time interval 14.8–13.5 Ma (middle Early Badenian to early Late Badenian). Periods of volcanic activity alternated with breaks of variable duration represented by internal erosion surfaces and unconformities. The stratovolcano reached a diameter of 35 to 40 km at the base of the volcanic cone and a probable elevation of 3000 to 4000 m.

3. Construction of the compound stratovolcano was followed by a period of denudation and emplacement of the extensive subvolcanic intrusive complex of diorite, granodiorite,

granodiorite porphyry and quartz-diorite porphyry during the time interval 13.5–12.9 Ma (Late Badenian). The youngest quartz-diorite sills were emplaced at the time of the initial subsidence of the Štiavnica Caldera.

4. Subsidence of the Štiavnica Caldera accompanied by activity of differentiated biotite-amphibole andesites occurred during the time interval 13.1–12.7 Ma (late Late Badenian). Volcanic activity overlapped partially with the emplacement of the youngest quartz-diorite porphyry sills.

5. Renewed explosive and effusive activity of andesites at centers in the caldera and on the slopes of the stratovolcano occurred during the time interval 12.7–12.2 Ma (Early Sarmatian).

6. Resurgent horst uplift accompanied by rhyolite volcanic activity along marginal faults took place during the time interval 12.2–11.4 Ma (Late Sarmatian to earliest Pannonian). Uplift of the resurgent horst and activity of the associated epithermal system continued till 10.7 Ma (Early Pannonian).

7. Sporadic activity of high alumina basalts in the northern sector of the stratovolcano took place during the time interval 11.1–8.2 Ma (Early to Late Pannonian).

8. Sporadic activity of alkali basalts took place in the time interval 7.8–7.2 Ma and 0.5–0.25 Ma. The younger age as reported on the basis of the position above one of the Quaternary terraces and OSL dating of underlying sedimentary rocks is problematic.

The lifespan of the stratovolcano is apparently shorter than assumed earlier. It was active in the interval 15.0 to 11.4 Ma (middle Early Badenian to earliest Pannonian), hydrothermal activity of the late stage epithermal system extending for 1.3 Myr since 12.0 till 10.7 Ma. Periods of volcanic/magmatic activity were separated by breaks of variable duration represented by unconformities and related denudation.

Our success in isotope dating of the granodiorite/diorite pluton and differentiated rocks filling the caldera enabled an indirect dating of associated mineralizations. Results obtained from rhyolites confirm association of the extensive late stage epithermal systems with rhyolite magmatism.

We have confirmed that K-Ar dating of groundmass fraction combined with Rb-Sr isochron dating in the cases of possible rejuvenation provides highly reliable results even in the case of complex evolution and deeply eroded volcanoes with exposed subvolcanic intrusions and related hydrothermal systems. The precision of the Rb-Sr method "internal" isochrones applied to Neogene volcanic rocks is limited by in-homogeneity of the initial $^{87}Sr/^{86}Sr$ ratios in mineral components. Nevertheless, in most cases when the Rb-Sr method was applied to dating the volcanic and intrusive rocks of the Štiavnica Stratovolcano, it has provided reliable results with precision of ± 0.2–0.5 Ma.

Acknowledgments: This study has been carried out in the framework of the Russian-Slovak scientific cooperation between the Institute of Geology of Ore Deposits, Petrography, Mineralogy and Geochemistry of the Russian Academy of Sciences, Moscow and the Geological Institute of the Slovak Academy of Sciences, Bratislava, project "Genetic and chronological relations of magmatism and epithermal ore genesis in the Neogene volcanostructures, Central Slovakia" (2008–2011). The authors appreciate support by the VEGA Grant 2/0162/11, Slovakia and Russian Foundation of Basic Research Grants 09-05-00870, 10-05-00354. Our thanks also go to our colleagues Dr. M. Háber and Ing. R. Kaňa for their assistance during the sample collection in field. We are grateful to anonymous reviewers for their constructive remarks that helped to improve the presentation of our results.

References

Bagdasarjan G.P., Konečný V. & Vass D. 1970: Contribution of absolute ages to the evolutionary scheme of Neogene volcanics of Central Slovakia. *Geol. Práce, Spr.* 51, 47–69 (in Slovak).

Baksi A.K. 1982: A note on the calculation of errors in conventional K-Ar dating. *Chem. Geol.* 35, 167–172.

Baksi A.K., York D. & Watkins N.D. 1967: Age of the Steens Mountain geomagnetic polarity transition. *J. Geophys. Res.* 72, 6299–6308.

Balogh K., Mihaliková A. & Vass D. 1981: Radiometric dating of basalts in southern and central Slovakia. *Západ. Karpaty, Ser. Geol. (GÚDŠ Bratislava)* 7, 113–126.

Balogh K., Konečný V. & Lexa J. 1998: K-Ar dating of the youngest calc-alkali rocks in the Central Slovakia Neogene Volcanic Field. *Abstract*, *XVIth congress CBGA,* Vienna, 59.

Brestenská E. 1970: Neogene sediments from the sheet Levice 1:50,000. *Open file report, Archive ŠGÚDŠ,* Bratislava, 1–68 (in Slovak).

Brestenská E., Konečný V., Lexa J. & Priechodská Z. 1980: Geological map 1:25,000 and explanatory notes — sheets Tekovské Trsťany and Hontianske Tesáre. *Open file report, Archive ŠGÚDŠ,* Bratislava, 1–133 (in Slovak).

Chernyshev I.V., Háber M., Kovalenker V.A., Ivanenko V.V., Jeleň S. & Karpenko M.I. 1995: To the age position of the magmatic events and epithermal Au-Ag-base metals mineralization in the central zone of the Banská Štiavnica Stratovolcano: K-Ar data. *Geol. Carpathica* 46, 6, 327–334.

Chernyshev I.V., Arakelyants M.M., Lebedev V.A. & Bubnov S.N. 1999: K-Ar isotope systematics and age of lavas from the Quaternary Kazbek Volcanic Province, Greater Caucasus. *Doklady Earth Sci.* 367A, 6, 862–866.

Chernyshev I.V., Kraus I., Kovalenker V.A., Goltsman Yu.V. & Lebedev V.A. 2000: Isotope Rb-Sr and K-Ar time constraints for activity of epithermal fluid-magmatic systems: Banská Štiavnica and Kremnica case. *Miner. Slovaca* 32, 247–248.

Chernyshev I.V., Lebedev V.A., Bubnov S.N., Arakelyants M.M. & Goltsman Yu.V. 2001: Stages of magmatic activity in the Elbrus Volcanic Center (Greater Caucasus): Evidence from isotope-geochronological data. *Doklady Earth Sci.* 380, 7, 384–389.

Chernyshev I.V., Lebedev V.A., Bubnov S.N., Arakelyants M.M. & Goltsman Yu.V. 2002: Isotopic geochronology of Quaternary volcanic eruptions in the Greater Caucasus. *Geochem. Int.* 40, 11, 1042–1055.

Chernyshev I.V., Lebedev V.A. & Arakelyants M.M. 2006: K-Ar dating of Quaternary volcanics: methodology and interpretations of results. *Petrology* 14, 1, 62–80.

Čechovič V. & Vass D. 1962: Problem of Tortonian strata subdivision in surroundings of Modrý Kameň. *Geol. Práce, Spr.* 25, 160–182 (in Slovak).

Harzhauser M. & Piller W.E. 2007: Benchmark data of a changing sea — Palaeogeography, palaeobiogeography and events in the Central Paratethys during the Miocene. *Palaeogeogr. Palaeoclimatol. Palaeoecol.* 253, 8–31.

Háber M., Jeleň S., Kovalenker V.A. & Černyšev I.V. 2001: Model of epithermal ore mineralization of the Banská Štiavnica ore district. *Miner. Slovaca* 33, 215–224 (in Slovak).

Kantor J. & Ďurkovičová J. 1985: Genetic characteristics of selected mineralizations in Western Carpathians. *Open file report, Archive ŠGÚDŠ,* Bratislava (in Slovak).

Kantor J. & Wiegerová V. 1981: Radiometric ages of selected basalts in Slovakia by $^{40}Ar/^{40}K$ method. *Geol. Zbor. Geol. Carpath.* 32, 29–34 (in Slovak).

Kantor J., Ďurkovičová J., Eliáš K., Repčok I., Ferenčíková E., Hašková A., Kovářová A., Rúčka I. & Sládková M. 1988: Isotopic research of metallogenetic processes. Part I. The area Rudno–Brehy–Pukanec. *Open file report, Archive ŠGÚDŠ,* Bratislava, 1–145 (in Slovak).

Kantor J., Ďurkovičová J., Sládková M. & Wiegerová V. 1990: Radiometric dating of selected rock complexes by K-Ar method. *Open file report, Archive ŠGÚDŠ,* Bratislava, 1–36 (in Slovak).

Kantorová V. 1962: Results of microbiostratigraphic studies of Tertiary marine sediments from the map sheet Modrý Kameň. *Open file report, Archive ŠGÚDŠ,* Bratislava (in Slovak).

Karátson D., Márton E., Harangi Sz., Józsa S., Balogh K., Pécskay Z., Kovácsvölgy S., Szakmány G. & Dulai A. 2000: Volcanic evolution and stratigraphy of the Miocene Börzsöny Mountains, Hungary: an integrated study. *Geol. Carpathica* 51, 325–343.

Karolus K. & Váňová M. 1973: Beziehung der sarmatischen Sedimente zu den Neovulkaniten der Mittleren Slowakei. *Geol. Práce, Spr.* 61, 155–182.

Karolus K., Karolusová E., Vozár J., Brestenská E., Priechodská Z., Škvarka L., Ritter J. & Kušík M. 1975: Complex evaluation of the structural borehole PKŠ-1 Gondovo. *Open file report, Archive ŠGÚDŠ,* Bratislava, 1–141 (in Slovak).

Koděra P. & Lexa J. 2003: Position of the Au deposit Hodruša in the geologic and metallogenetic evolution of the Štiavnica Stratovolcano (Slovakia). In: Ellopoulos et al. (Eds.): Mineral exploration and sustainable development. *CD-ROM, Millpress (Rotterdam)*, 1189–1192.

Koděra P., Rankin A.H. & Lexa J. 1998: Evolution of fluids responsible for iron skarn mineralisation: an example from the Vyhne-Klokoč deposit, Western Carpathians, Slovakia. *Miner. Petrology* 64, 119–147.

Koděra P., Lexa J., Rankin A.H. & Fallick A.E. 2004: Fluid evolution in a subvolcanic granodiorite pluton related to Fe and Pb-Zn mineralization, Banská Štiavnica ore district, Slovakia. *Econ. Geol.* 99, 1745–1770.

Koděra P., Lexa J., Rankin A.H. & Fallick A.E. 2005: Epithermal gold veins in a caldera setting: Banská Hodruša, Slovakia. *Mineralium Depos.* 39, 921–943.

Koděra P., Lexa J., Fallick A.E., Biroň A., Gregor M., Uhlík M. & Kraus I. 2010: Tracing low sulphidation systems from their roots down to foothills — example from the Kremnica ore and industrial minerals fields (Slovakia). *Acta Mineral. Petrogr., Abstr. Ser.* 6, 289.

Konečný P. 2002: Magmatic evolution of the Štiavnica Stratovolcano. *Unpublished PhD Thesis, Comenius University,* Bratislava (in Slovak).

Konečný V. 1970: Evolution of Neogene volcanic complexes in the Štiavnické vrchy mountain range. *Geol. Práce, Spr.* 51, 5–46 (in Slovak).

Konečný V. 1971: Evolutionary stages of the Banská Štiavnica Caldera and its post-volcanic structures. *Bull. Volcanol.* XXXV, 95–116.

Konečný V. & Lexa J. 2001: Structure and evolution of the Štiavnica Stratovolcano. *Miner. Slovaca* 33, 179–196 (in Slovak).

Konečný V., Planderová E., Ondrejíčková A., Lehotayová R., Klablenová K. & Škvarka L. 1966: Final report on the structural borehole GK-3 Rykynčice. *Open file report, Archive ŠGÚDŠ,* Bratislava, 1–57 (in Slovak).

Konečný V., Bagdasarjan G.P. & Vass D. 1969: Evolution of Neogene volcanism in central Slovakia and its confrontation with absolute ages. *Acta Geol. Acad. Sci. Hung.* 13, 245–258.

Konečný V., Lexa J. & Planderová E. 1983: Stratigraphy of the Central Slovakia Neogene Volcanic Field. *Západ. Karpaty, Sér. Geol.* 9, 1–203 (in Slovak with English summary).

Konečný V., Lexa J. & Hók J. 1993: Geological map of the central zone of Štiavnica Stratovolcano in the scale 1:10,000. *Open file report, Archive ŠGÚDŠ,* Bratislava, 1–138 (in Slovak).

Konečný V., Lexa J. & Hojstričová V. 1995: The Central Slovakia Neogene volcanic field: a review. In: Downes H. & Vaselli O. (Eds.): Neogene and related magmatism in the Carpatho-Pannonian region. *Acta Volcanol.* 7, 63–78.

Konečný V., Lexa J., Halouzka R., Hók J., Vozár J., Dublan L., Nagy A., Šimon L., Havrila M., Ivanička J., Hojstričová V., Mihaliková A., Vozárová A., Konečný P., Kováčiková M., Filo M., Marcin D., Klukanová A., Liščák P. & Žáková E. 1998: Explanatory notes to the geological map of Štiavnické vrchy and Pohronský Inovec mountain ranges (Štiavnica Stratovolcano). *Geol. Surv. SR,* Bratislava, 1–473 (in Slovak with English summary).

Konečný V., Lexa J. & Balogh K. 1999: Neogene–Quaternary alkali basalt volcanism in Central and Southern Slovakia (Western Carpathians). *Geolines* 9, 67–75.

Kovalenker V.A., Jeleň S., Levin K.A., Naumov V.B., Prokofjev V.J. & Rusinov V.L. 1991: Mineral assemblages and physical-chemical model of the formation of gold-silver-polymetallic mineralisation on the deposit Banská Štiavnica (Central Slovakia). *Geol. Carpathica* 42, 291–302.

Kovalenker V.A., Naumov V.B., Prokofjev V.Yu., Jeleň S. & Háber M. 2006: Composition of magmatic melts and evolution of mineral-forming fluids in the Banská Štiavnica Epithermal Au-Ag-Pb-Zn Deposit, Slovakia: A study of inclusions in minerals. *Geochem. Int.* 44, 2, 118–136.

Kováč M., Fordinál K., Grigorovich A.S.A., Halásová E., Hudáčková N., Joniak P., Pipík R., Sabol M., Kováčová M. & Sliva Ľ. 2005: Western Carpathian fossil ecosystems and their relationship to paleoenvironment in the context of Euro-Asian continent Neogene evolution. *Geol. Práce, Spr.* 111, 61–121 (in Slovak).

Kraus I., Chernyshev I.V., Šucha V., Kovalenker V.A., Lebedev V.A. & Šamajová E. 1999: Use of illite for K-Ar dating of hydrothermal precious and base metal mineralization in Central Slovak Neogene Volcanic Rocks. *Geol. Carpathica* 50, 5, 1–12.

Kráľ J., Lexa J. & Koděra P. 2002: Isotope geochemistry of the Štiavnica Stratovolcano mineralizations. In: Lexa et al. (Eds.): Metallogenetic evaluation of the Slovak Republic territory. *Open file report, Archive ŠGÚDŠ,* Bratislava, 1–10 (in Slovak).

Lehotayová R. 1964: Microfauna of Miocene sediments at the southern margin of the Central Slovakia Neogene Volcanic Field. *Správy o Geol. Výskumoch v r. 1963, Geol. Ústav D. Štúra,* Bratislava 2, 12–13 (in Slovak).

Lexa J. 2001: Metallogeny of the Štiavnica Stratovolcano. *Miner. Slovaca* 33, 203–214 (in Slovak).

Lexa J. & Konečný V. 1988: Geodynamic aspects of the Neogene to Quaternary volcanism. In: Rakús M. (Ed.): Geodynamic development of the Western Carpathians. *Geol. Surv. Slovak Republic,* Bratislava, 219–240.

Lexa J. & Pécskay Z. 2010: Radiometric dating of rhyolites by conventional K-Ar method: methodical aspects. In: Kohút M. (Ed.): Dating of minerals and rocks, metamorphic, magmatic and metallogenetic processes, as well as tectonic events. *ŠGÚDŠ,* Bratislava, 21–22.

Lexa J., Štohl J. & Konečný V. 1999a: Banská Štiavnica ore district: relationship among metallogenetic processes and the geological evolution of a stratovolcano. *Mineralium Depos.* 34, 639–665.

Lexa J., Štohl J. & Žáková E. 1999b: The Šobov high-sulfidation system. In: Molnár F., Lexa J. & Hedenquist J.W. (Eds.): Epithermal mineralization of the Western Carpathians. *Soc. Econ. Geol., Guid. Ser.* 31, 259–264.

Lexa J., Halouzka R., Havrila M., Hanzel V., Kubeš P., Liščák P. & Hojstričová V. 1998a: Explanatory notes to the geological map of Kremnické vrchy mountain range. *Geol. Surv. Slovak Republic,* Bratislava, 1–308 (in Slovak with English summary).

Lexa J., Konečný P., Hojstričová V., Konečný V. & Köhlerová M. 1998b: Petrologic model of the Štiavnica Stratovolcano, Central Slovakia Neogene Volcanic Field. *Abstract, XVIth Congress CBGA,* Vienna, 1– 340.

Matsumoto A. & Kobayashi T. 1995: K-Ar age determination of late Quaternary volcanic rocks using the "mass fractionation correction procedure": application to the Younger Ontake Volcano, central Japan. *Chem. Geol.* 125, 123–135.

Onačila D., Lexa J., Marsina K., Rojkovičová Ľ., Káčer Š., Hojstričová V., Žáková E., Štohl J., Konečný V., Nemčok M., Koděra P., Konečný P., Repčok I., Hurai V., Háber M., Jeleň S., Maťo Ľ., Sasvári T., Schmidt R., Zvara I. & Grant T. 1995: Metallogenetic model and resource assessment of the Štiavnica Stratovolcano central zone. *Open file report, Archive ŠGÚDŠ,* Bratislava, 1–231 (in Slovak).

Ozdínová S. 2008: Badenian calcareous nannofossils from Semerovce ŠV-8 and Cífer-1 boreholes (Danube Basin). *Miner. Slovaca* 40, 141–150.

Papp A. 1963: Die Biostratigraphische Gliederung des neogens im Wiener Becken. *Mitt. Geol. Gesell. (Wien)* 56, 225–317.

Pécskay Z., Lexa J., Szakács A., Seghedi I., Balogh K., Konečný V., Zelenka T., Kovacs M., Póka T., Fülöp A., Márton E., Panaiotu C. & Cvetković V. 2006: Geochronology of Neogene-Quaternary magmatism in the Carpathian arc and Intra-Carpathian area: a review. *Geol. Carpathica* 57, 511–530.

Planderová E. 1990: Miocene microflora of Slovak central Paratethys and its biostratigraphic significance. *Dionýz Štúr Inst. Geol.,* Bratislava, 1–144.

Repčok I. 1978: Ages of selected rocks in the Central Slovakia Volcanic Field by Uranium fission track method. *Geol. Práce, Spr.* 71, 69–76.

Repčok I. 1979: Dating of rocks in the Central Slovakia Volcanic Field by fission track method. *Open file report, Archive ŠGÚDŠ,* Bratislava, 1–33 (in Slovak).

Repčok I. 1980: New data on age of the Štiavnica Stratovolcano rocks by fission track method. *Geol. Práce, Spr.* 74, 185–187 (in Slovak).

Repčok I. 1981: Dating of rocks in the Central Slovakia Volcanic Field by Uranium fission track method. *Západ. Karpaty, Sér. Mineral. Petrogr. Geochém. Metalogen.* 8, 59–104 (in Slovak).

Repčok I. 1982: Dating of Neogene volcanics in Western Carpathians by Uranium fission track method. *Open file report, Archive ŠGÚDŠ,* Bratislava (in Slovak).

Repčok I. 1984: Dating of Neogene volcanics in Western Carpathians. In: Kantor J. et al.: Time evolution in selected areas of the Western Carpathians. *Open file report, Archive ŠGÚDŠ,* Bratislava, 1–176 (in Slovak).

Sillitoe R. 2010: Porphyry copper systems. *Econ. Geol.* 105, 3–41.

Singer B.S., Wijbrans J.R., Nelson S.T., Pringle M.S., Feeley T.C. & Dungan M.A. 1998: Inherited argon in a Pleistocene andesite lava: ^{40}Ar/^{39}Ar incremental-heating and laser-fusion analyses of plagioclase. *Geology* 26, 427–430.

Sitár V. 1973: Die Fossile Flora sarmatischer Sedimenten aus der Umgebung von Močiar in der mittleren Slowakei. *Acta Geol. Geogr. Univ. Comen., Geol.* 26, 5–85.

Smith R.L. & Bailey R.A. 1968: Resurgent cauldrons. In: Coats R.R., Hay R.L. & Anderson C.A. (Eds.): Studies in volcanology. *Geol. Soc. Amer. Mem.* 116, 153–210.

Steiger R.H. & Jäger E. 1977: Subcommission on geochronology: convention on the use of decay constants in geo- and cosmochronology. *Earth Planet. Sci. Lett.* 36, 359–362.

Šimon L. & Halouzka R. 1996: Pútikov vŕšok volcano — the youngest volcano in the Western Carpathians. *Geol. Mag.* 2, 96, 103–123.

Šimon L. & Maglay J. 2005: Dating of sediments underlying the Putikov vŕšok volcano lava flow by the OSL method. *Miner. Slovaca* 37, 279–281 (in Slovak with English summary).

Štohl J. 1976: Mineralizations of the Central Slovakia Volcanic Field related to the central-Carpathian lineament. *Západ. Karpaty, Sér. Mineral., Petrogr., Geochém., Metalogen.* 2, 7–40 (in Slovak with English summary).

Vass D. & Balogh K. 1989: The period of main and late Alpine molasses. *Z. Geol. Wiss. Berlin* 17, 849–858.

Vass D., Konečný V. & Šefara J. 1979: Geology of the Ipeľ basin and Krupina plateau. *Geol. Ústav D. Štúra,* Bratislava, 1–277 (in Slovak with English summary).

Vass D., Brestenská E., Fejdiová O., Franko O., Gazda S., Lehotayová R., Marková M., Ondrejičková A., Planderová E., Reichwalder P. & Vozárová A. 1981: Structural borehole ŠV-8 (Dolné Semerovce). *Regionálna Geol. Záp. Karpát, (GÚDŠ Bratislava)* 14, 1–106 (in Slovak).

Appendix 1

New K-Ar data for rocks of the Štiavnica Stratovolcano.

No.	Sample	Rock type	Fraction	K (%) ± σ	$^{40}Ar_{rad}$ (ng/g) ± σ	$^{40}Ar_{atm}$ (%)	Age (Ma) ± 2σ
Volcanic formations pre-dating Štiavnica Stratovolcano							
1	GP-4	px-amph andesite with garnet	plag	0.454 ± 0.004	0.460 ± 0.005	41.4	14.6 ± 0.4
			gdm	**2.19 ± 0.03**	**2.289 ± 0.009**	**9.6**	**15.0 ± 0.4**
Lower structural unit (1st stage)							
2	GK-2/01	Px andesite	gdm	1.80 ± 0.02	1.907 ± 0.010	12.6	15.2 ± 0.4
3	GK-111	Amph-px andesite	**gdm**	**1.83 ± 0.02**	**1.880 ± 0.007**	**12.6**	**14.8 ± 0.3**
4	GK-110	Amph-px andesite	plag	0.288 ± 0.003	0.312 ± 0.003	37.3	15.6 ± 0.5
			gdm	**2.07 ± 0.03**	**2.013 ± 0.011**	**22.5**	**14.0 ± 0.4**
5	St-6/06	Amph-px andesite	**gdm**	**1.44 ± 0.02**	**1.407 ± 0.005**	**6.7**	**14.0 ± 0.4**
6	St-4/06	Px andesite matrix	**gdm**	**1.61 ± 0.02**	**1.542 ± 0.016**	**24.4**	**13.8 ± 0.4**
7	St-5/06	Px andesite fragment	**gdm**	**1.84 ± 0.03**	**1.762 ± 0.007**	**6.6**	**13.8 ± 0.4**
8	GK-107	Px andesite	**gdm**	**1.83 ± 0.02**	**1.801 ± 0.009**	**20.5**	**14.1 ± 0.3**
9	GK-106	Px andesite	**plag**	**0.421 ± 0.004**	**0.404 ± 0.003**	**34.2**	**13.8 ± 0.4**
			gdm	**2.57 ± 0.03**	**2.460 ± 0.009**	**11.3**	**13.7 ± 0.3**
10	GP-13	Px andesite	**gdm**	**2.27 ± 0.03**	**2.121 ± 0.008**	**12.8**	**13.4 ± 0.4**
11	St-7/06	Px andesite	**gdm**	**2.90 ± 0.03**	**2.740 ± 0.012**	**23.5**	**13.5 ± 0.3**
12	St-14/06	Px andesite	**gdm**	**2.67 ± 0.03**	**2.510 ± 0.020**	**74.0**	**13.5 ± 0.4**
13	GK-57	Px andesite	plag	0.158 ± 0.002	0.165 ± 0.003	73.4	15.1 ± 0.7
			gdm	**2.15 ± 0.03**	**1.982 ± 0.014**	**71**	**13.2 ± 0.4**
14	GP-11	Px andesite	plag	0.260 ± 0.003	0.213 ± 0.004	71.4	11.8 ± 0.5
			gdm	**2.22 ± 0.03**	**2.031 ± 0.010**	**35.7**	**13.1 ± 0.4**
Middle structural unit (caldera filling, 3rd stage)							
19	GK-100	Px-bt-amph andesite	**gdm**	**1.85 ± 0.02**	**1.682 ± 0.010**	**22.9**	**13.1 ± 0.3**
20	GK-16	Bt-amph andesite	plag	0.259 ± 0.003	0.273 ± 0.003	39.4	15.1 ± 0.5
			bt	**7.02 ± 0.08**	**6.23 ± 0.02**	**19.1**	**12.8 ± 0.3**
			gdm	2.76 ± 0.03	2.27 ± 0.02	36.3	11.8 ± 0.3
21	GK-20	Px-bt-amph andesite	**plag**	**0.279 ± 0.003**	**0.252 ± 0.003**	**46.5**	**13.0 ± 0.4**
			bt	6.04 ± 0.07	5.08 ± 0.04	76.1	12.1 ± 0.3
			gdm	2.85 ± 0.03	2.345 ± 0.010	41.1	11.8 ± 0.3
Upper structural unit (4th stage)							
22	St-9/06	Px andesite	**gdm**	**2.60 ± 0.03**	**2.285 ± 0.013**	**14.2**	**12.6 ± 0.3**
23	St-10/06	Px andesite	**gdm**	**3.35 ± 0.04**	**2.914 ± 0.013**	**17.2**	**12.5 ± 0.3**
24	GK-105	Bt-amph-px andesite	plag	0.307 ± 0.012	0.328 ± 0.005	60	15.4 ± 0.6
			gdm	**3.18 ± 0.04**	**2.818 ± 0.011**	**20.2**	**12.7 ± 0.3**
26	St-1/06	Px andesite	**gdm**	**2.55 ± 0.03**	**2.291 ± 0.011**	**13.5**	**12.9 ± 0.3**
27	St-11/06	Px andesite ± bt	**gdm**	**3.55 ± 0.04**	**3.203 ± 0.013**	**14.4**	**13.0 ± 0.3**
28	St-12/06	Amph-px andesite ± bt	**gdm**	**3.61 ± 0.04**	**3.102 ± 0.016**	**56.6**	**12.4 ± 0.3**
29	St-15/06	Px andesite	**gdm**	**2.58 ± 0.03**	**2.195 ± 0.009**	**8.5**	**12.2 ± 0.3**
30	St-16/06	Amph-px andesite	**gdm**	**2.93 ± 0.03**	**2.451 ± 0.011**	**9.6**	**12.0 ± 0.3**
Rhyolites of the Jastrabá Formation (5th stage)							
32	GK-21	Rhyolite	plag	0.257 ± 0.003	0.245 ± 0.002	17.9	13.7 ± 0.4
			bt	**6.79 ± 0.07**	**5.79 ± 0.02**	**35.3**	**12.2 ± 0.3**
			gdm	**4.48 ± 0.05**	**3.712 ± 0.013**	**16.7**	**11.9 ± 0.3**
33	KSD-1	Rhyolite	**gdm**	**8.00 ± 0.09**	**6.42 ± 0.02**	**34.2**	**11.5 ± 0.3**
Post-rhyolite volcanic formations — alkali basalts							
40	S-B3/02	Nepheline basanite	**gdm**	**1.50 ± 0.02**	**0.047 ± 0.001**	**82.4**	**0.45 ± 0.03**
41	S-B7/02	Nepheline basanite	**gdm**	**1.32 ± 0.02**	**0.038 ± 0.002**	**89.9**	**0.42 ± 0.03**
42	S-B8/02	Nepheline basanite	**gdm**	**1.05 ± 0.02**	**0.031 ± 0.001**	**80.4**	**0.43 ± 0.03**

Results considered as reliable (see text) are indicated by bold letters on grey background. Dated mineral fraction abbreviations: **plag** — plagioclase, **bt** — biotite, **gdm** — groundmass.

Appendix 2

Table: The Rb-Sr isotope data and isochrone ages for rocks of the Štiavnica Stratovolcano.

No.	Sample	Rock type	Fraction	Rb (ppm)	Sr (ppm)	$^{87}Rb/^{86}Sr \pm 2\sigma$	$^{87}Sr/^{86}Sr \pm 2\sigma$	Isochron age (Ma ± 2σ)
Subvolcanic/intravolcanic intrusive complexes (2nd stage)								
15	St-5/99	Granodiorite	w.r.	165	382	1.2514 ± 28	0.706937 ± 14	**13.4 ± 0.2**
			plag	86	790	0.3167 ± 9	0.706790 ± 13	I_0 = 0.70668 ± 0.00011
			kfs	470	360	3.753 ± 9	0.707464 ± 14	MSWD = 10.1
			bt I	420	27	45.24 ± 21	0.715240 ± 30	
			bt II	512	15.6	94.98 ± 47	0.724741 ± 12	
16	St-2/04	Granodiorite	w.r.	176	396	1.282 ± 3	0.706899 ± 13	**13.3 ± 0.6**
			plag	53	800	0.1911 ± 5	0.706533 ± 14	I_0 = 0.70668 ± 0.00036
			kfs	456	337	3.911 ± 10	0.707456 ± 13	MSWD = 71
			bt I	422	37	32.901 ± 9	0.713167 ± 14	
			bt II	528	16	94.14 ± 45	0.724350 ± 12	
17	St-4/08	Diorite	w.r.	60	306	0.567 ± 2	0.708591 ± 10	**13.3 ± 0.2**
			plag	22	133	0.471 ± 3	0.708652 ± 13	I_0 = 0.70857 ± 0.00022
			amph	16	25	1.857 ± 9	0.709014 ± 20	MSWD = 26
			bt	450	6.1	215.3 ± 8	0.749253 ± 17	
17a	St-2/08	Quartz-diorite porphyry	w.r.	91	381	0.6876 ± 20	0.707093 ± 10	**(16–11)**
			plag	29	846	0.0975 ± 5	0.707226 ± 10	
			amph I	4.7	58	0.235 ± 2	0.707411 ± 12	
			amph II	5.5	62	0.259 ± 2	0.707337 ± 13	
			bt I	223	59	10.91 ± 6	0.709426 ± 11	
			bt II	212	213	2.888 ± 15	0.708360 ± 10	
			matrix	118	339	1.010 ± 3	0.707218 ± 9	
Middle structural unit (caldera filling, 3rd stage)								
18	St-83/91	Bt-amph andesite	plag	2.9	1079	0.00790 ± 12	0.706603 ± 16	**12.4 ± 0.1**
			amph	19	74	0.7479 ± 22	0.706754 ± 20	I_0 = 0.706612 ± 0.000025
			bt	458	32	41.30 ± 17	0.713873 ± 16	MSWD = 0.70
20	GK-16	Bt-amph andesite	w.r.	120	370	0.939 ± 2	0.707291 ± 14	**12.9 ± 0.5**
			plag	3.1	1125	0.00798 ± 21	0.706864 ± 18	I_0 = 0.70701 ± 0.00013
			amph	30	80	1.107 ± 3	0.707217 ± 14	MSWD = 28
			bt I	420	28	43.22 ± 11	0.714890 ± 20	
			bt II	376	43	25.12 ± 8	0.711653 ± 19	
			gdm	136	295	1.331 ± 3	0.707265 ± 13	
Upper structural unit (4th stage)								
24	GK-105	Bt-amph-px andesite	w.r.	74	330	0.6538 ± 15	0.706604 ± 13	**12.3 ± 0.2**
			bt	107	42	26.44 ± 7	0.711121 ± 17	I_0 = 0.70649 ± 0.00004
25	KSD-2	Bt-amph-px ignimbrite	w.r.	147	279	1.527 ± 4	0.706904 ± 14	**12.0 ± 0.2**
			plag	5.2	767	0.0195 ± 2	0.706574 ± 16	I_0 = 0.706628 ± 0.000071
			amph	3.8	73	0.1482 ± 7	0.706699 ± 20	MSWD = 6.1
			bt	387	21	54.40 ± 13	0.715879 ± 24	
			gdm	206	160	3.702 ± 9	0.707252 ± 16	
28	St-12/06	Amph-px andesite ± bt	w.r.	148	308	1.388 ± 3	0.705541 ± 10	**12.3 ± 0.7**
			plag	7	888	0.0227 ± 3	0.705257 ± 10	I_0 = 0.70531 ± 0.00019
			bt	430	31.4	39.76 ± 12	0.712273 ± 10	MSWD = 17
			gdm	218	190	3.305 ± 8	0.705975 ± 11	
Rhyolites of the Jastrabá Formation (5th stage)								
31	St-18/06	Rhyolite	w.r.	226	52	12.52 ± 3	0.708685 ± 14	**12.2 ± 0.8**
			kfs	147	290	1.469 ± 4	0.706605 ± 10	I_0 = 0.7064 ± 0.0011
			bt	480	7.5	184.3 ± 5	0.738288 ± 14	MSWD = 42
32	GK-21	Rhyolite	w.r.	195	116	4.869 ± 11	0.707271 ± 17	**10.5 ± 0.2**
			plag	3.6	165	0.0657 ± 10	0.706576 ± 20	I_0 = 0.70658 ± 0.00015
			bt	390	7.8	145.0 ± 4	0.728204 ± 36	MSWD = 8.9
			gdm	252	49	14.94 ± 4	0.708878 ± 18	
35	L-8/91	Rhyolite	bt	470	23	58.81 ± 26	0.716625 ± 11	**12.1 ± 0.1**
			glass	204	107	5.503 ± 16	0.707486 ± 13	I_0 = 0.70654 ± 0.00004
36	St-6/08B	Rhyolite	w.r.	206	153	3.901 ± 9	0.707313 ± 11	**11.8 ± 0.1**
			plag	10.7	936	0.0330 ± 3	0.706673 ± 14	I_0 = 0.706659 ± 0.000021
			bt	416	20.2	59.50 ± 18	0.716648 ± 10	MSWD = 0.28
			gdm	212	126	4.808 ± 12	0.707456 ± 11	

Mineral fractions: **w.r.** — whole rock, **plag** — plagioclase, **kfs** — K-feldspar, **amph** — amphibole, **bt** — biotite, **gdm** — groundmass.

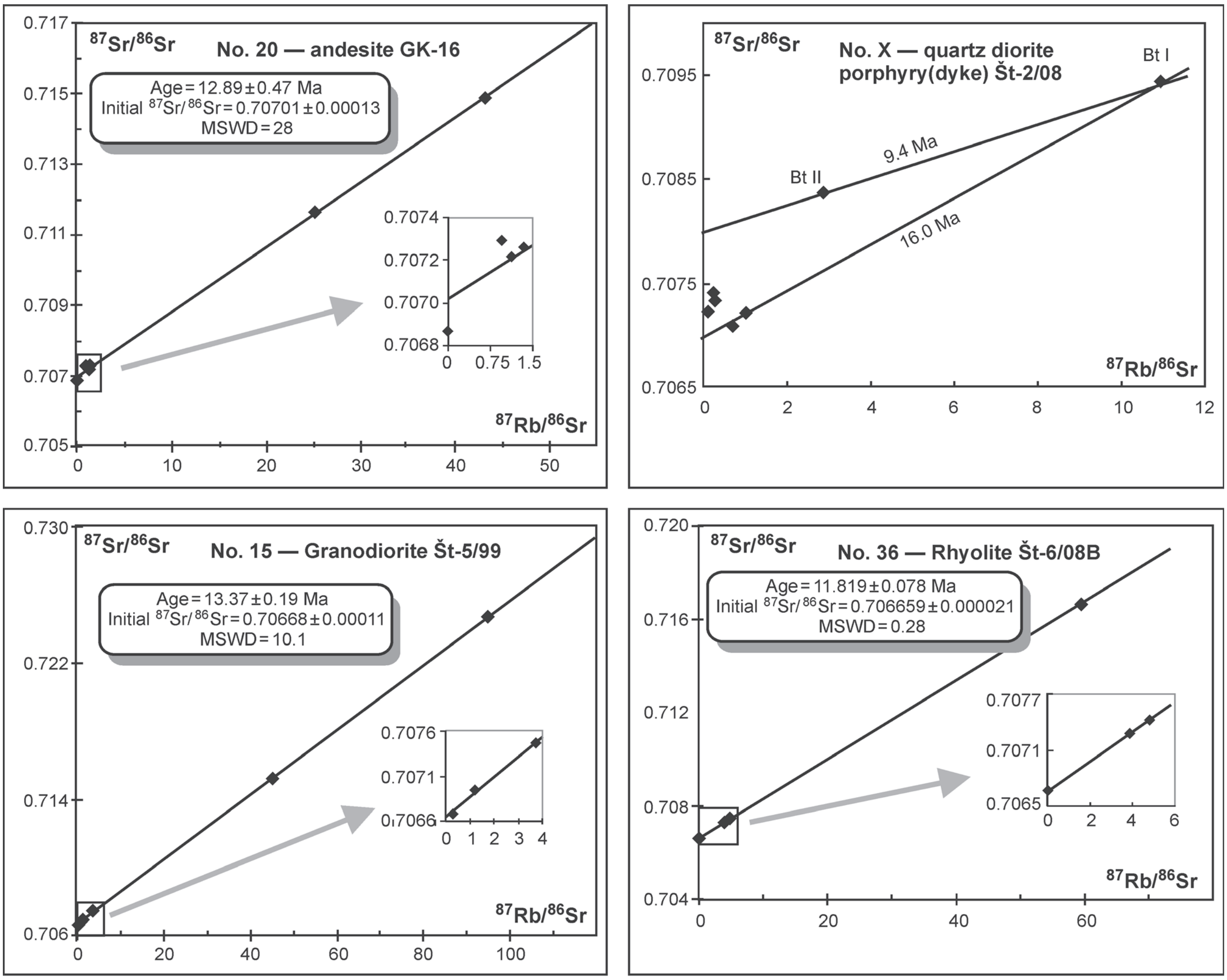

Fig. A. Rb-Sr isochrone plots for rocks of the Štiavnica Stratovolcano.

Appendix 3

Localization, geology and petrography of rock samples collected from lithostratigraphic units of the Štiavnica Stratovolcano for K-Ar and Rb-Sr dating.

For each of the dated samples there are given: number used throughout this paper including the Figure 2; original sample name; WGS 84 coordinates in the degree/minute/second format; localization in italic; geological position; petrographic description (mineral abbreviations: **Amf** – amphibole, **Bt** – biotite, **Cpx** – clinopyroxene (augite), **Gdm** – groundmass, **Gnt** – garnet, **Kfs** – K-feldspar, **Ol** – olivine, **Opx** – orthopyroxene (hypersthene), **Pl** – plagioclase, **Px** – pyroxene, **Q** – quartz).

Volcanic formations pre-dating Štiavnica Stratovolcano

1 GP-4 48 31 15.4 N 19 05 55.7 E	
Quarry at the Breziny settlement, SW of the city Zvolen.	
Lithostratigraphic unit: *Neresnica Formation*	
Geology:	Massive, blocky andesite with obscured banded texture from the internal part of the extrusive dome
Petrography:	Pyroxene–amphibole andesite with garnet
Phenocrysts:	Pl – 2–6 mm, 10–12 %, $An_{30–50}$; Amf – 3–8 mm, 10–11 %, opacitized; Px (glomeroporphyric grains) – 2.3 %; Gnt – 0.4–0.8 cm, 0.7 %
Groundmass:	Microhyalopilitic to micropilotaxitic
Alteration:	Low autometamorphic – chloritization, limonitization

Štiavnica Stratovolcano

Lower structural unit (1st stage)

2 GK–2/01 48 19 17.4 N 18 58 42.1 E	
Quarry bellow b.m. 408 Žarnosek, loc. Tepličky south of the village Prenčov, southern slope of the stratovolcano.	
Lithostratigraphic unit: undefined, position above the *Sebechleby Formation*	
Geology:	Lava flow with a well developed platy and blocky jointing fills up a N–S oriented paleovalley in rocks of the *Sebechleby Formation;* owing to its geological setting it was formerly assigned to lava flows of the upper structural unit
Petrography:	Pyroxene andesite
Phenocrysts:	Pl – 0.2–2 mm, 25–30 %, An_{50}; Cpx + Opx – 0.2–2 mm, 10 – 15 %; Q – 0.4 mm, rare
Groundmass:	Cryptocrystalline

3 GK–111 48 18 59.3 N 18 52 14.9 E	
Quarry south of the village Baďan, southern slope of the stratovolcano.	
Lithostratigraphic unit: *Sebechleby Formation*	
Geology:	Lava flow of massive andesite showing platy to blocky jointing
Petrography:	Amphibole–pyroxene andesite
Phenocrysts:	Pl – 0.5–2.5 mm, $An_{35–50}$; Opx + Cpx – 0.2–2 mm; Amf – rare, opacitized
Groundmass:	Hyalopilitic

4 GK–110 48 23 36.1 N 18 55 51.9 E	
Outcrop at the state road south of the village Sv. Anton, southern slope of the stratovolcano.	
Lithostratigraphic unit: *Sebechleby Formation*	
Geology:	Block in coarse to blocky epiclastic volcanic breccia; breccia laid down by a lahar makes up a thick horizon among andesite lava flows
Petrography:	Amphibole–pyroxene andesite
Phenocrysts:	Pl – 3–5 mm, 15 %, $An_{35–55}$; Px – 0.4–2.2 mm, 10 %, Cpx > Opx; Amf – up to 2 mm; Bt – rare
Groundmass:	Hyalopilitic

5 St–6/06 48 17 59.0 N 18 55 13.3 E	
Quarry bellow b.m. 529 Šibač, north of the village Sebechleby, southern slope of the stratovolcano.	
Lithostratigraphic unit: *Sebechleby Formation*	
Geology:	Lava flow formed of massive andesite with irregular blocky jointing
Petrography:	Amphibole–pyroxene andesite
Phenocrysts:	Pl – 0.5–3 mm, 3 %, An_{60}; Opx – 0.5–2 mm, 5–8 %; Amf – 0.3–2 mm, rare
Groundmass:	Hyalopilitic to microlitic

Appendix 3 *Continued*

6 St–4/06 48 21 39.6 N 18 57 52.7 E	
Outcrop at the forest road northwest of the village Královce–Krnišov, southeastern slope of the stratovolcano	
Lithostratigraphic unit: *undefined, position bellow rocks of the Sebechleby Formation*	
Geology:	Welded pyroclastic flow deposits or froth lava situated underneath block and ash pyroclastic flow breccias of the *Sebechleby Formation*
Petrography:	Pyroxene andesite, welded matrix of breccia
Phenocrysts:	Pl – 1–2 mm, An$_{30–35}$; Opx – 2 mm; Cpx – 0.5 mm
Groundmass:	recrystallized, micropoikilitic
Alteration:	Partial oxidation

7 St–5/06 48 21 39.6 N 18 57 52.7 E	
Outcrop at the forest road northwest of the village Královce–Krnišov, southeastern slope of the stratovolcano	
Lithostratigraphic unit: undefined, position *bellow rocks of the Sebechleby Formation*	
Geology:	Fragment in welded pyroclastic flow deposits or froth lava situated under–neath block and ash pyroclastic flow breccias of the *Sebechleby Formation*
Petrography:	Pyroxene andesite
Phenocrysts:	Pl – up to 1.2 mm, 20 %, An$_{40–60}$; Cpx – 0.6 mm, 5–8 %; Opx – 0.8 mm, 5–8 %
Groundmass:	Microphelsitic, locally micropoikilitic

8 GK–107 48 23 59.8 N 18 57 11.1 E	
Small quarry at the state road Sv. Anton – Žibritov, southeastern slope of the stratovolcano	
Lithostratigraphic unit: *Žibritov Effusive Complex*	
Geology:	Lava flow of massive andesite shows lamination and platy jointing; it rests upon the eroded surface of the *Sebechleby Formation*
Petrography:	Pyroxene andesite
Phenocrysts:	15–25 %, Pl >Px; Pl – up to 2 mm, An$_{40–70}$; Opx – up to 1 mm, Cpx □– up to 0.8 mm
Groundmass:	Hyalopilitic

9 GK–106 48 24 00.6 N 18 56 52.7 E	
Outcrop at the forest road west of the village Žibritov, southeastern slope of the stratovolcano	
Lithostratigraphic unit: *Žibritov Effusive Complex*	
Geology:	Lava flow of massive andesite shows lamination and platy jointing; it rests upon the eroded surface of the *Sebechleby Formation*
Petrography:	Pyroxene andesite
Phenocrysts:	20 %, Pl >Px; Pl – up to 1.5 mm, 10–12 %, An$_{25–40}$; Opx; Cpx; Bt – rare
Groundmass:	Hyalopilitic

10 GP–13 48 23 51.3 N 19 05 17.0 E	
Cliff bellow the hill Mäsiarsky bok north of the town Krupina, eastern slope of the stratovolcano	
Lithostratigraphic unit: *Žibritov Effusive Complex*	
Geology:	Lava flow of massive andesite shows lamination and platy jointing
Petrography:	Pyroxene andesite
Phenocrysts:	35 %, Pl/Px = 2/1; Pl – up to 0.3–0.5 mm, An$_{35}$; Opx – up to 2.5 mm; Cpx; Amph – 0.3–0.5 mm, rare
Groundmass:	Hyalopilitic, locally micropoikilitic

11 St–7/06 48 22 35.2 N 19 02 13.5 E	
Quarry Ficberg northwest of the town Krupina, eastern slope of the stratovolcano	
Lithostratigraphic unit: *Žibritov Effusive Complex*	
Geology:	Lava flow of massive andesite showing platy or columnar jointing; it rests on rocks of the *Sebechleby Formation*
Petrography:	Pyroxene andesite
Phenocrysts:	25 %; Pl – up to 1.5 mm, 15 %, An$_{60–65}$; Opx – up to 1 mm, Cpx – up to 1 mm
Groundmass:	Hyalopilitic

12 St–14/06 48 24 47.9 N 18 26 40.1 E	
Abandoned quarry next to the village Machulince, lower one of two lava flows, northwestern slope of the stratovolcano	
Lithostratigraphic unit: top of the lower structural unit	
Geology:	Andesite lava flow associated with hyaloclastite breccias; it has been formerly assigned to the *Inovec Formation* of the fourth stage (Konečný et al. 1998) without any specific arguments
Petrography:	Pyroxene andesite
Phenocrysts:	15–20 %; Pl – 1–3 mm, An$_{30–35}$; Opx; Cpx
Groundmass:	Hyalopilitic

Appendix 3 *Continued*

13 GK–57	**48 24 53.1 N 18 26 48.0 E**
Abandoned quarry next to the village Machulince, upper one of two lava flows, northwestern slope of the stratovolcano	
Lithostratigraphic unit: top of the lower structural unit	
Geology:	Andesite lava flow associated with hyaloclastite breccias; it has been formerly assigned to the *Inovec Formation* of the fourth stage (Konečný et al. 1998) without any specific arguments
Petrography:	Pyroxene andesite
Phenocrysts:	15 %, Pl >Px; Pl – 2.3 mm, $An_{45–55}$; Px – up to 1.2 mm, Cpx > Opx
Groundmass:	Cryptocrystalline

14 GP–11	**48 22 58.6 N 18 37 38.7 E**
Outcrop in the valley southeast of the village Tekovská Breznica, western slope of the stratovolcano	
Lithostratigraphic unit: middle part of the lower structural unit	
Geology:	Lava flow of massive andesite showing irregular blocky jointing
Petrography:	Pyroxene andesite
Phenocrysts:	30 %, Pl/Px = 1/1; Pl – up to 2,5 mm, $An_{35–50}$; Px – up to 2,5 mm, Opx > Cpx
Groundmass:	Microlitic locally microlite–hyalopilitic

Subvolcanic/intravolcanic intrusive complexes (2nd stage)

15 St–5/99	**48 27 11.0 N 18 46 48.2 E**
Small quarry near the Mayer shaft, Hodruša Valley, western part of the resurgent horst	
Lithostratigraphic unit: *Hodruša–Štiavnica Intrusive Complex*	
Geology:	Granodiorite pluton, roughly 50 – 100 m below its former roof; it is partially affected by propylitic alteration
Petrography:	Equigranular granodiorite, hypidiomorphic–granular texture, grains 4–5 mm
Minerals:	Hypidiomorphic grains of Pl – $An_{40–51}$, Bt, Amf; allotriomorphic grains of Kfs, Q; rare apatite, titanite, zircon, magnetite, tourmaline
Alteration:	Propylitization – albitization of Pl, sericite, carbonate, pyrite, secondary quartz

16 St–2/04	**48 27 18.9 N 18 46 22.7 E**
Outcrop next to gallery entrance, Sandrik in the Hodruša Valley, western part of the resurgent horst	
Lithostratigraphic unit: *Hodruša–Štiavnica Intrusive Complex*	
Geology:	Granodiorite pluton, roughly 50 – 100 m below its former roof; it is partially affected by propylitic alteration
Petrography:	Equigranular granodiorite, hypidiomorphic–granular texture, grains 4–5 mm
Phenocrysts:	Hypidiomorphic grains of Pl – $An_{40–51}$, Bt, Amf; allotriomorphic grains of Kfs, Q; rare apatite, titanite, zircon, magnetite, tourmaline
Alteration:	Propylitization – albitization of Pl, sericite, carbonate, pyrite, secondary quartz

17 St–4/08	**48 29 12.6 N 18 51 05.7 E**
Pivná dolina Valley, northwest of the village Banky, northern part of the resurgent horst	
Lithostratigraphic unit: *Hodruša–Štiavnica Intrusive Complex*	
Geology:	Diorite intrusion at the northern side of the granodiorite pluton, roughly 100 m below the former roof
Petrography:	Equigranular diorite, hypidiomorphic–granular texture, grains 1–2 mm
Minerals:	Hypidiomorphic grains of Pl – An $_{55–72}$, Cpx, Amf, minor Bt; minor allotriomorphic grains of Q and Kfs
Alteration:	Weak propylitization

17a St–2/08	**48 25 20.7 N 18 48 30.1 E**
Road–cut in the Richňava Valley, 1 km south of the settlement Banisko, western part of the resurgent horst	
Lithostratigraphic unit: *Banisko Intrusive Complex*	
Geology:	Dyke crosscutting andesites of the Lower structural unit; the rock is slightly affected by regional propylitization
Petrography:	Quartz–diorite porphyry
Phenocrysts:	35 %; Pl, Amf, Bt, rare Q
Groundmass:	Microallotriomorphic granular
Alteration:	Weak propylitization

Appendix 3 *Continued*

Middle structural unit (3rd stage)

18 St–83/91 48 27 18.9 N 18 56 34.8 E	
Barlangi quarry next to the settlement Kysihýbel, east of the town Banská Štiavnica, southeastern part of the caldera	
Lithostratigraphic unit: *Studenec Formation*	
Geology:	The internal part of a large extrusive dome; massive to slightly porous andesite of reddish color shows blocky jointing and a weak autometamorphic alteration; the locality is quite close the outer zone of argillic alterations related to the extensive system of younger epithermal veins
Petrography:	Biotite–amphibole andesite
Phenocrysts:	40 %, up to 5 mm; Pl – $An_{15–35}$; Amf, Opx, Q
Groundmass:	Glassy, locally microspherulitic
Alteration:	Weak oxidation

19 GK–100 48 24 54.8 N 18 53 19.0 E	
Cliff on to northeastern slope of the hill Sitno, southwest of the village Ilija, southern part of the caldera	
Lithostratigraphic unit: *Studenec Formation*	
Geology:	Thick lava flow of massive andesite with blocky jointing; the lava flow is in the upper part of the formation; the locality is not affected by younger hydrothermal processes
Petrography:	Pyroxene–biotite –amphibole andesite
Phenocrysts:	20–25 %, Pl, Amf>Bt, Opx; Pl – 1.5–2 mm, $An_{15–35}$; Amf – 0.8 mm, Bt – 0.7–3 mm; Opx – up to 0.8 mm
Groundmass:	Glassy, locally partially spherulitic

20 GK–16 48 30 43.9 N 18 54 39.6 E	
Cliff northwest of the village Podhorie, eastern part of the caldera	
Lithostratigraphic unit: *Studenec Formation*	
Geology:	The marginal part of an extrusive dome; the locality is outside of the zone affected visibly by younger hydrothermal processes
Petrography:	Biotite-amphibole andesite
Phenocrysts:	30–35 %, mostly Pl; Pl – 3–3.5 mm, $An_{25–40}$; Amf – 2.5–3 mm; Bt – 0.5–3.5 mm
Groundmass:	Spherulitic–microlitic, locally passing into hyalopilitic to microlitic

21 GK–20 48 32 40.6 N 18 56 34.8 E	
Outcrop in the roadcut north of the village Močiar, northeastern part of the caldera	
Lithostratigraphic unit: *Studenec Formation*	
Geology:	The internal part of an extrusive dome; the locality is outside of the zone affected visibly by younger hydrothermal processes
Petrography:	Pyroxene–biotite–amphibole andesite
Phenocrysts:	20–25 %; Pl – up to 4.5 mm, $An_{30–65}$,10–15 %; Amf – up to 3.5 mm; Bt – up to 1.5 mm; Opx – 0.8 mm;
Groundmass:	Hyalomicrolitic

Upper structural unit (4th stage)

22 ST–9/06 48 13 16.6 N 18 46 41.4 E	
Quarry next to Kamenný chotár, southeast of the village Žemberovce, southwestern slope of the stratovolcano	
Lithostratigraphic unit: *Baďan Formation*	
Geology:	Andesite lava flow showing blocky to platy jointing; the lava flow associates with hyaloclastite breccia
Petrography:	Pyroxene andesite
Phenocrysts:	10–15 %, Pl>Amf>Px; Pl – 1.5 mm, $An_{40–60}$; Amf, Px – rare
Groundmass:	Pilotaxitic, partially glassy

23 ST–10/06 48 13 30.0 N 18 40 22.1 E	
Quarry next to the village Krškany, southwestern slope of the stratovolcano	
Lithostratigraphic unit: *Baďan Formation*	
Geology:	Andesite lava flow showing blocky to platy jointing; the lava flow associates with hyaloclastite breccia
Petrography:	Pyroxene andesite
Phenocrysts:	15–20 %, mostly Pl; Pl – 1–2 mm, $An_{60–70}$; Amf – rare, Px – rare
Groundmass:	Hyalopilitic, locally micropoikilitic

Appendix 3 *Continued*

24 GK–105 48 23 37.1 N 18 55 08.8 E	
Cliff at the top of Biely Kameň Hill, north of the village Prenčov, southeastern part of the caldera	
Lithostratigraphic unit: *Sitno Effusive Complex*	
Geology:	Andesite with blocky jointing represents the central part of a thick lava flow; the lava flow filled originally a paleovalley at the top of caldera filling in the southern part of the Štiavnica Caldera
Petrography:	Biotite–amphibole–pyroxene andesite
Phenocrysts:	10–15 %; Pl – up to 3 mm, $An_{45–60}$, 8–10 %; Amf – 0.8 mm, opacitized; Bt – up to 3–3.5 mm
Groundmass:	Hyalopilitic

25 KSD–2 48 25 43.8 N 18 39 48.1 E	
Cliffs in the slope above the river Hron, 1.5 km east of the town Nová Baňa, eastern slope of the stratovolcano	
Lithostratigraphic unit: *Drastvica Formation*	
Geology:	Andesitic ignimbrite is strongly welded, almost homogenized. Fiamme as well as other oriented texture are obscured. The sample represents the central part of roughly 100 m thick ignimbrite flow with un–welded pumice tuffs at the base. Ignimbrite is not affected by hydrothermal alteration, however, west of the locality there is an extensive extrusive dome of younger rhyolite.
Petrography:	Biotite–amphibole–pyroxene andesitic ignimbrite
Phenocrysts:	45 – 50 %; Pl, Px, Amf, Bt
Groundmass:	Devitrified, cryptocrystalline, pseudofluidal structure

26 St–1/06 48 35 05.2 N 18 59 48.6 E	
Small quarry at the road south of the village Hronská Dúbrava, northern slope of the stratovolcano	
Lithostratigraphic unit: upper part of the *Breznica Complex*	
Geology:	Lava flow – massive andesite with blocky to platy jointing
Petrography:	Pyroxene andesite
Phenocrysts:	25–30 %, mostly Pl; Pl – up to 3 mm, $An_{35–55}$; Opx –up to 3 mm, Cpx – up to 2 mm
Groundmass:	Hyalopilitic

27 St–11/06 48 16 55.4 N 18 29 51.6 E	
Quarry northwest of the village Malé Kozmálovce, western slope of the stratovolcano	
Lithostratigraphic unit: *Priesil Formation*	
Geology:	Andesite lava flow passing laterally into hyaloclastite breccias
Petrography:	Pyroxene andesite with rare biotite
Phenocrysts:	25 %, mostly Pl; Pl – 2.5 mm, $An_{40–60}$, 15 %; Cpx – 0.4–1.5 mm, Opx, Bt – rare
Groundmass:	Hyalopilitic, locally micropoikilitic

28 St–12/06 48 18 17.3 N 18 31 52.2 E	
Quarry next to the village Kozárovce, southwestern slope of the stratovolcano	
Lithostratigraphic unit: *Priesil Formation*	
Geology:	Andesite lava flow passing laterally into hyaloclastite breccias
Petrography:	Amphibole–pyroxene andesite with minor biotite
Phenocrysts:	15 %; Pl – up to 2.5 mm, $An_{40–60}$, 8–10 %; Px – up to 1 mm, Amf – 0.7 mm, Bt – 1.5 mm
Groundmass:	Hyalopilitic

29 St–15/06 48 24 01.3 N 18 28 14.6 E	
Quarry at the ridge Krivá 4 km southeast of the village Machulince, western slope of the stratovolcano	
Lithostratigraphic unit: *Inovec Formation*	
Geology:	Lava flow – gray massive andesite showing lamination and well developed platy jointing
Petrography:	Pyroxene andesite
Phenocrysts:	20 %, mostly Pl; Pl – up to 1.4 mm; Opx – up to 1.2 mm, Cpx – 0.5 mm, Amf – 0.6 mm, opacitized, rare
Groundmass:	Hyalopilitic to microlitic

30 St–16/06 48 34 14.3 N 18 38 01.8 E	
Cliff at the slope of the hill Klenový vrch, 2 km west of the village Ostrý Grúň, northwestern slope of the stratovolcano	
Lithostratigraphic unit: *Žiar Effusive Complex*	
Geology:	Lava flow of massive andesite showing blocky to platy jointing
Petrography:	Amphibole–pyroxene andesite
Phenocrysts:	35 %, mostly Pl; Pl – up to 2.5 mm, $An_{40–65}$; Px – up to 2.5 mm, Amf – 0.5 mm, opacitized
Groundmass:	Hyalopilitic to pilotaxitic

Appendix 3 *Continued*

Rhyolites of the Jastrabá Formation (5th stage)

31 St–18/06 48 26 24.3 N 18 58 35.0 E	
Outcrop at the field road south of the village Banský Studenec, southeastern part of the caldera	
Lithostratigraphic unit: *Jastrabá Formation*	
Geology:	Dyke emplaced along the Štiavnica Caldera fault
Petrography:	Rhyolite
Phenocrysts:	15–20 %; Q – up to 2 mm; Pl – 1.5 mm, Kfs, Bt – 1–1.3 mm
Groundmass:	Spherulitic

32 GK–21 48 33 23.5 N 18 56 42.7 E	
Outcrop 2 km north of the village Močiar, northern part of the caldera	
Lithostratigraphic unit: *Jastrabá Formation*	
Geology:	The central part of a 25 m thick N–S oriented dyke with blocky jointing; the dyke crosscuts rocks of the *Studenec Formation* and a lava flow of the *Sitno Effusive Complex*
Petrography:	Rhyolite
Phenocrysts:	30 %; Q – up to 2 mm; Pl – 3.5 mm, $An_{35–55}$; Kfs – 2.5 mm, Bt – 2 mm
Groundmass:	Felsitic with transition to micropoikilitic

33 KSD–1 48 26 47.8 N 18 38 49.9 E	
Northern Štamproch quarry, north of the town Nová Baňa, northwestern part of the stratovolcano	
Lithostratigraphic unit: *Jastrabá Formation*	
Geology:	The marginal part of an extensive extrusive dome. Rhyolite at the sampling site is not visibly affected by hydrothermal alteration. However, visible alteration of the Nová Baňa epithermal system starts about 500 m south of the sampling site. K_2O content 9.11 % (Appendix 2) implies K-metasomatism (adularization?).
Petrography:	Rhyolite
Phenocrysts:	20–25 %; Q – 2.5 mm; Kfs – 4.5 mm, Bt – 2 mm, partly altered
Groundmass:	Felsitic with transition to mikropoikilitic
Alteration:	Adularization

34 V–7/91c 48 30 33.7 N 18 47 30.0 E	
Cliffs above stone sea west of the town Vyhne, western part of the resurgent horst	
Lithostratigraphic unit: *Jastrabá Formation*	
Geology:	The central part of a cryptodome emplaced along marginal faults of the resurgent horst in the center of the Štiavnica Caldera; rhyolite is affected by subsolidus recrystallization and K-metasomatism – K_2O content is 10.38 % (Appendix 2)
Petrography:	Rhyolite
Phenocrysts:	35 %; Pl – mostly replaced by adularia, Q – 2.5 mm; Kfs – 4.5 mm, Bt – altered to chlorite
Groundmass:	Felsitic
Alteration:	Subsolidus recrystallization + adularization, chloritization of Bt

35 L–8/91 48 32 24.1 N 18 48 36.7 E	
Perlite quarry next to the village Lehôtka pod Brehmi, northwestern edge of the resurgent horst	
Lithostratigraphic unit: *Jastrabá Formation*	
Geology:	Perlite block in hyaloclastite breccia; hyaloclastite breccia associates with extrusive dome situated at the fault zone between the resurgent horst and Žiar Depression
Petrography:	Glassy rhyolite – perlite
Phenocrysts:	10 %, 1–2 mm; Pl, Bt
Groundmass:	Hyaline, locally vesicular

36 St–6/08B 48 32 24.1 N 18 48 36.7 E	
Perlite quarry next to the village Lehôtka pod Brehmi, northwestern edge of the resurgent horst	
Lithostratigraphic unit: *Jastrabá Formation*	
Geology:	Perlite block in hyaloclastite breccia; hyaloclastite breccia associates with extrusive dome situated at the fault zone between the resurgent horst and Žiar Depression
Petrography:	Glassy rhyolite – perlite
Phenocrysts:	Pl – 1.7 mm, 8 %; Bt – 1 mm, 7 %; Pl and Bt form glomeroporphyric aggregates
Groundmass:	Hyaline

Appendix 3 *Continued*

37 Kl–1/91 48 27 40.4 N 18 54 36.9 E	
Klotilda vein at the12th level of New Shaft, Banská Štiavnica; eastern side of the resurgent horst	
Lithostratigraphic unit: *Jastrabá Formation*	
Geology:	Rhyolite dyke invading a base metal rich epithermal vein structure; it is affected by strong hydrothermal alteration
Petrography:	Rhyolite
Phenocrysts:	15 %; Kfs, minor Q, pseudomorphoses of adularia after Pl, altered Bt
Groundmass:	Aggregate of secondary Q and adularia with pyrite grains (0.5–1 %)
Alteration:	Adularization, silicification + pyrite

Post-rhyolite volcanic formations – alkali basalts

38 St–84/91 48 27 40.0 N 18 56 16.5 E	
Abandoned quarry at the side of railroad next to the settlement Kysihýbel, east of the town Banská Štiavnica	
Lithostratigraphic unit: *Alkali basalts*	
Geology:	Nepheline basanite lava neck – the lava part of a volcanic pipe
Petrography:	Nepheline basanite
Phenocrysts:	Around 40 %; Pl, Cpx, Ol
Groundmass:	Fine-grained
Alteration:	Zeolites in vesicules

39 St–85/91 48 27 42.6 N 18 54 51.3 E	
Cliff at the southern side of the Kalvária Hill, eastern side of the town Banská Štiavnica	
Lithostratigraphic unit: *Alkali basalts*	
Geology:	Lava neck – remnant of a lava lake in the former maar crater
Petrography:	Nepheline basanite
Phenocrysts:	Fine-grained
Groundmass:	45 %; Pl, Cpx, Ol, minor Bt

40 S–B3/02 48 24 13.5 N 18 38 02.0 E	
Quarry next to the road west of the village Brehy, south of the town Nová Baňa	
Lithostratigraphic unit: *Alkali basalts*	
Geology:	Lava flow of massive basanite with blocky to columnar jointing
Petrography:	Nepheline basanite
Phenocrysts:	Pl rare, Px rare, Ol – 0.8 mm, minor Bt
Groundmass:	Fine-grained with glass and microlites of Pl, Ol, Cpx, magnetite, ilmenite

41 S–B7/02 48 22 37.0 N 18 38 14.8 E	
Cliff at the southwestern side of Pútikov vŕšok Hill, east of the village Tekovská Breznica	
Lithostratigraphic unit: *Alkali basalts*	
Geology:	Sample comes from a basanite lava neck in the central part of a scoria cone
Petrography:	Nepheline basanite
Phenocrysts:	10 %; Ol – 0.5–0.6 mm; rare Cpx
Groundmass:	Fine-grained with glass and microlites of Pl, Ol, Cpx, ore minerals, vesicules are rimed by plagioclase microlites

42 S–B8/02 48 22 29.4 N 18 38 25.6 E	
Outcrop at the southern side of Pútikov vŕšok Hill, east of the village Tekovská Breznica	
Lithostratigraphic unit: *Alkali basalts*	
Geology:	Sample comes from a thin basanite lava flow at the foot of a scoria cone
Petrography:	Nepheline basanite
Phenocrysts:	10 %; Ol – 1.1–3 mm, rare Pl, Cpx
Groundmass:	Hyaline, porous, showing transitions into hyalopilitic

Appendix 4

Major element composition (wt. %) of Štiavnica Stratovolcano dated rocks.

No.	Sample	SiO_2	TiO_2	Al_2O_3	Fe_2O_3	MnO	MgO	CaO	Na_2O	K_2O	P_2O_5	S	LOI	Total
Volcanic formation pre-dating Štiavnica Stratovolcano														
1	GP - 4	62.48	0.71	14.69	7.24	0.148	2.35	5.16	2.62	2.13	0.173		0.85	98.55
Lower structural unit (1st stage)														
2	GK - 2/01	60.60	0.58	17.36	6.24	0.112	1.69	6.44	2.78	1.58	0.111	0.01	1.31	98.81
3	GK - 111	60.25	0.68	17.37	6.49	0.105	1.28	6.57	2.69	1.61	0.106	0	1.34	98.49
4	GK - 110	62.44	0.57	16.63	5.31	0.082	1.24	6.37	2.57	1.52	0.097	0.01	1.09	97.93
5	St - 6/06	56.35	0.78	19.16	7.81	0.133	3.56	7.21	2.86	1.40	0.149		0.05	99.46
6	St - 4/06	56.45	0.86	18.52	8.36	0.18	3.58	6.73	2.82	1.50	0.129		0.66	99.79
7	St - 5/06	57.24	0.80	18.79	7.66	0.110	2.82	6.48	2.92	1.65	0.138		1.16	99.77
8	GK - 107	58.74	0.87	16.58	7.41	0.105	1.62	6.61	2.57	1.77	0.122	0	1.38	97.78
9	GK - 106	63.02	0.63	16.45	5.98	0.092	1.38	5.24	2.48	2.60	0.153	0.01	0.27	98.31
10	GP - 13	60.74	0.91	15.33	7.40	0.117	2.75	5.72	2.41	2.49	0.149		0.84	98.86
11	St - 7/06	57.72	0.83	17.12	7.67	0.130	3.83	6.54	2.61	2.33	0.178		0.70	99.66
12	St - 14/06	57.87	1.06	19.25	6.46	0.101	1.62	6.85	2.81	2.68	0.307		0.75	99.76
13	GK - 57	59.68	1.28	16.70	7.23	0.104	1.65	6.13	2.90	2.39	0.272		0.90	99.24
14	GP - 11	60.30	0.85	14.94	7.86	0.145	3.88	5.78	2.34	2.11	0.156		1.37	99.73
Subvolcanic/intravolcanic intrusive complexes (2nd stage)														
15	St - 5/99	62.45	0.65	15.57	5.69	0.118	2.41	4.57	2.73	3.52	0.19		1.87	97.90
16	St - 2/04	63.90	0.66	15.66	5.48	0.091	2.50	4.56	2.68	3.56	0.18		0.52	99.27
17	St - 4/08	56.47	0.78	16.90	8.32	0.137	4.60	7.36	2.44	1.52	0.15		0.96	99.64
Middle structural unit (caldera filling, 3rd stage)														
19	GK - 100	65.43	0.46	14.91	4.88	0.082	1.60	4.99	2.03	2.46	0.168	0.02	1.44	98.47
20	GK - 16	65.93	0.58	14.56	4.90	0.095	2.17	4.55	2.32	2.71	0.178		1.85	99.84
21	GK - 20	65.73	0.53	15.48	4.99	0.097	1.82	4.48	2.15	2.85	0.136		2.45	100.71
Upper structural unit (4th stage)														
22	St - 9/06	56.99	0.91	19.62	6.19	0.118	0.94	7.13	3.28	2.43	0.245		1.56	99.41
23	St - 10/06	63.72	0.91	16.28	5.99	0.035	0.36	3.41	3.69	3.61	0.256		1.37	99.63
24	GK - 105	62.30	0.70	16.82	6.96	0.123	1.91	6.74	2.55	1.64	0.127	0.01	0.80	100.68
25	KSD - 2	69.36	0.62	14.47	2.84	0.024	0.59	3.72	2.43	3.26	0.112		1.18	98.61
26	St - 1/06	56.77	0.91	18.01	7.68	0.107	3.78	6.51	2.83	1.90	0.217		1.09	99.80
27	St - 11/06	58.60	0.96	17.32	6.85	0.113	1.50	5.70	3.37	3.37	0.236		1.73	99.75
28	St - 12/06	65.58	0.72	15.55	4.46	0.05	1.29	4.58	3.13	3.22	0.208		0.92	99.71
29	St - 15/06	59.23	0.69	17.64	7.21	0.172	2.83	5.73	2.98	2.19	0.198		0.77	99.64
30	Št - 16/06	58.66	0.82	17.50	7.45	0.126	3.13	5.88	2.79	2.34	0.198		0.97	99.86
Rhyolites of the Jastrabá Formation														
31	St - 18/06	73.73	0.14	13.96	1.85	0.016	0.28	0.48	2.08	5.15	0.010		2.12	99.82
32	GK - 21	77.80	0.12	11.77	1.16	0.022	0.21	1.08	2.50	4.64	0.018		0.82	100.14
33	KSD - 1	72.90	0.14	12.59	1.26	0.012	0.03	0.57	1.12	9.11	0.014		0.53	98.28
34	V - 7/91c	70.98	0.30	14.30	0.36	0.012	0.06	1.12	0.76	10.38	0.020		1.48	98.29
35	L - 8/91	71.36	0.22	13.57	1.70	0.043	0.34	1.30	2.55	5.13	0.040		3.37	99.62
36	St - 6/08B	70.81	0.26	13.78	1.95	0.043	0.43	1.44	2.41	5.20	0.060		3.24	99.62
Post-rhyolite volcanic formations – alkali basalts														
38	St - 84/91	48.12	2.65	16.73	11.43	0.162	5.67	8.59	4.00	1.54	0.520		0.46	99.41
39	St- 85/91B	46.52	2.69	14.21	11.49	0.159	10.22	9.02	3.05	1.21	0.430		0.84	99.00
40	S - B3/02	45.61	2.39	14.43	10.59	0.16	6.60	9.27	4.07	1.93	0.693		1.27	97.01
41	S - B7/02	46.70	2.23	15.13	9.65	0.145	6.53	9.70	3.98	1.77	0.731		1.68	98.25
42	S - B8/02	45.43	2.61	13.96	11.73	0.172	9.90	10.32	2.58	1.21	0.526		1.31	99.75

Appendix 4 *Continued*

Comments: Composition of the sample No. 1, representing garnet-bearing andesites pre-dating Štiavnica Stratovolcano, overlaps with the array of samples No. 2–14, representing the lower structural unit of the stratovolcano. This array lays almost completely in the field of andesites, only two samples No. 5 and 6 lay in the field of basaltic andesite in respect of the silica contents (Fig. B). On other side, volcanic rocks of the middle structural unit (caldera filling) correspond to dacite. Rocks of the upper structural unit No. 22–30 show compositions from andesite up to dacite and as a whole are slightly enriched in alkalies, especially Potassium. Analysed samples of subvolcanic intrusions No. 15–17 show diorite–granodiorite trend. (Fig. B). Composition of rhyolites No. 31–36 corresponds to high-potassium trend with moderate variations of silica content. Two of analysed rhyolite samples No. 33 and 34 show very high K_2O and low Na_2O contents as a result of hydrothermal adularization. Alkali basalt samples No. 38–42 project close to the boundaries of basalt, trachybasalt and basanite fields (Fig. B).

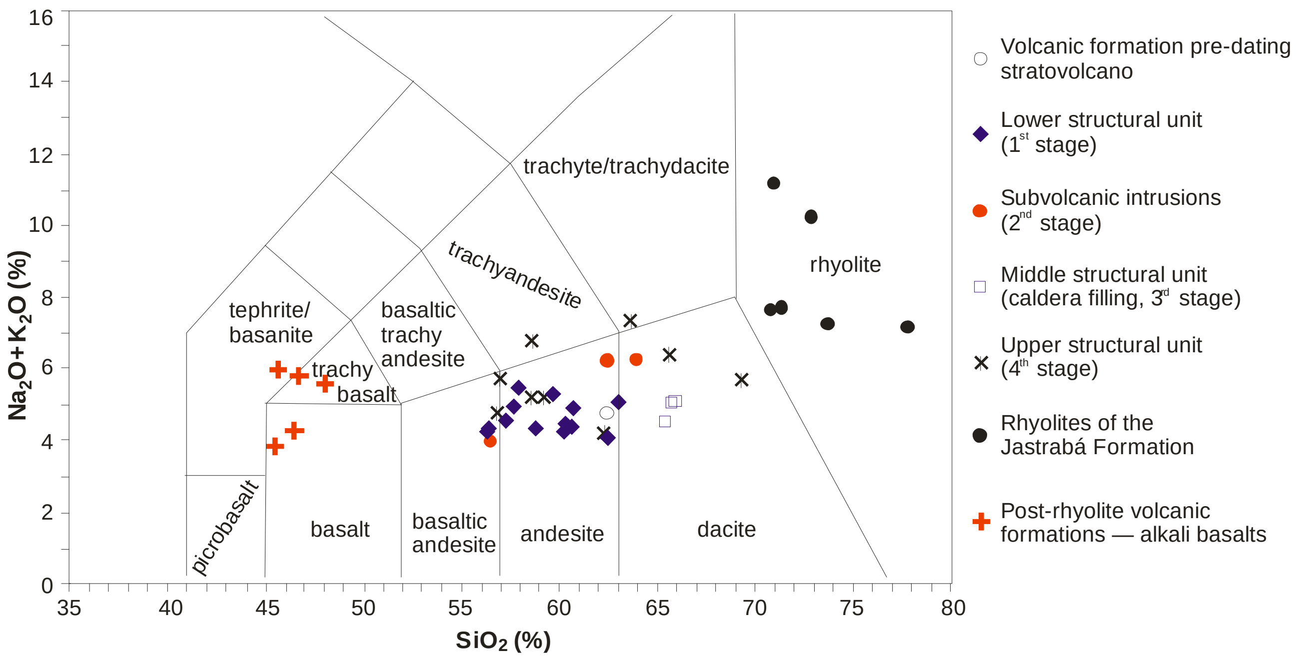

Fig. B. TAS plot for dated rocks of the Štiavnica Stratovolcano.